

cp3-bench: A tool for benchmarking symbolic regression algorithms tested with cosmology

M. E. Thing and S. M. Koksang

CP3-Origins, University of Southern Denmark, Campusvej 55, DK-5230 Odense M, Denmark

E-mail: thing@cp3.sdu.dk, koksang@cp3.sdu.dk

Abstract. We present a benchmark study of ten symbolic regression algorithms applied to cosmological datasets. We find that the dimension of the feature space as well as precision of datasets are highly important for symbolic regression tasks to be successful. We find no indication that inter-dependence of features in datasets are particularly important, meaning that it is not an issue if datasets e.g. contain both z and $H(z)$ as features. We find no indication that performance of algorithms on standardized datasets are good indications of performance on cosmological datasets. This suggests that it is not necessarily prudent to choose which symbolic regressions algorithm to use based on their performance on standardized data. Instead, a more prudent approach is to consider a variety of algorithms.

Overall, we find that most of the benched algorithms do rather poorly in the benchmark and suggest possible ways to proceed with developing algorithms that will be better at identifying ground truth expressions for cosmological datasets.

As part of this publication we introduce our benchmark algorithm cp3-bench which we make publicly available at <https://github.com/CP3-Origins/cp3-bench>. The philosophy behind cp3-bench is that it should be as user-friendly as possible, available in a ready-to-use format, and allow for easy additions of new algorithms and datasets.

Contents

1	Introduction	1
2	Cosmological datasets	2
2.1	Hubble data	3
2.2	Redshift drift in standard cosmology	3
2.3	Cosmic backreaction and two-region models	4
2.3.1	Redshift drift in 2-region models	7
2.4	Summary of data sets	8
3	Benchmarking with cosmological datasets	9
3.1	Benchmarking method	10
3.1.1	Framework	10
3.1.2	Getting started	12
3.1.3	Benchmark procedure	13
3.2	Benchmarking results: Cosmological datasets	16
4	Summary, discussion and conclusions	20
A	Standard datasets	21
B	Detailed results	23

1 Introduction

A core aspect of physics is that we are able to use symbolic expressions to describe how the world around us works. It is therefore a significant challenge when we meet a physical system, observable, or an experimental dataset that we cannot describe through mathematical formulas. This problem arises in various places in astrophysics and cosmology where, for instance, the precise halo mass function is unknown [1], stellar density profiles are estimated based on various approximations but the true underlying relation is yet to be discovered [2], a derived expression for the non-linear matter power spectrum does not yet exist [3, 4], and intricacies of general relativity leave useful expressions for observables such as the mean redshift drift [5, 6] still waiting to be found (the concept of mean redshift drift will be introduced in section 2). When a ground truth expression for an quantity is desired but seems unfeasible to obtain through analytical considerations, one option is to try to use symbolic regression which is a regression method based on machine learning (ML). Symbolic regression is, at least in principle, a powerful tool for identifying unknown relations between physical quantities such as data from astrophysical observations or laboratory experiments. When utilizing symbolic regression algorithms in e.g. cosmology, the approach has generally been to use one or very few specific algorithms. For instance, the work in [5, 6] utilized the symbolic regression algorithm AI Feynman [7, 8] because of its user-friendliness and because it was developed by physicists with discovering physics formulae in mind, showing an improvement compared to earlier state-of-the-art algorithms. The work presented in [3, 4] instead utilized OPERON [9] which was chosen due to its speed, memory efficiency and because it is based

on genetic algorithms which tend to do well in symbolic regression benchmark studies and competitions (e.g. [10, 11]).

In general, when we choose an algorithm for symbolic regression, we naturally make a decision we expect represents the state-of-the-art for the task. However, symbolic regression algorithms are usually evaluated and compared by studying their efficiency at identifying symbolic expressions corresponding to certain ensembles of datasets such as the Penn Machine Learning Benchmarks [12, 13], collections of mathematical expressions (see e.g. appendix A of [14]), simple physical laws as in EmpiricalBench of [15], and some even use a dataset based on equations from the Feynman Lectures on Physics [16], the so-called Feynman Symbolic Regression Database¹. Although these ensembles often do include physics datasets (not the least the Feynman Symbolic Regression Database), this does not necessarily mean that the resulting benchmark is particularly enlightening when it comes to the applicability of symbolic regression algorithms to real cosmology/astrophysics symbolic regression tasks. One hindrance is that real world cosmology problems are typically based on very complex physics which means that the corresponding datasets can be difficult to obtain, understand and can end up being complicated from a physical point of view, e.g. including several dependent variables. This type of dataset simply does not seem to be represented significantly in common machine learning/symbolic regression databases.

It is not clear that symbolic regression algorithms optimized with typical machine learning database problems are automatically also optimized for real world cosmology problems. We therefore here present a benchmark of symbolic regression algorithms based on specific cosmological datasets. While typical benchmark tasks can consist of hundreds of datasets, we here restrict the benchmark to only 19 datasets which are, however, genuine (synthetic) cosmological datasets related to and representing genuine symbolic regression tasks in cosmology.

To do the benchmark we have developed a new benchmark tool which we call cp3-bench. The version released together with this paper supports the ten different symbolic regression algorithms which are benchmarked in this paper. We provide cp3-bench in a ready-to-use format for Linux machines where installation and usage is straightforward.

In Section 2 below, we introduce the datasets we used for our benchmark, including an introduction to the cosmological settings they represent. In Section 3 we present the benchmark setup, our benchmark tool cp3-bench, example wrapper Things-to-bench and our results. Section 4 provides a summary and discussion of future possible developments.

2 Cosmological datasets

This section serves to describe the data used in our benchmark. In the first subsection below, we introduce the Hubble relation of standard cosmology. The subsequent subsection is dedicated to the observable known as redshift drift and its Friedmann-Lemaître-Robertson-Walker (FLRW) limit. In the final two subsections we introduce a specific family of toy cosmological models called two-region models and discuss how to compute the redshift drift as well as a quantity known as cosmic backreaction in these models. The datasets are summarized in Section 2.4 which includes a list of the datasets in Table 1.

¹<https://space.mit.edu/home/tegmark/aifeynman.html>

2.1 Hubble data

The Hubble parameter describes the expansion history of the Universe and has great interest in cosmology. Earlier work on symbolic regression such as [17, 18] has thus fittingly included showcasing the use of new symbolic regression algorithms for astrophysics by applying them to Hubble data either directly, or indirectly through supernova data. We will also use Hubble datasets here.

In the Λ CDM model, the Hubble parameter is given by

$$\frac{H^2(z)}{H_0^2} = \Omega_{m,0}(1+z)^3 + (1 - \Omega_{m,0}). \quad (2.1)$$

Using this relation, we have generated three different Hubble datasets. The first two are similar to those used in [17, 18] since we only consider a single cosmological model, namely the (flat) Λ CDM model with $H_0 = 70\text{km/s/Mpc}$ and $\Omega_{m,0} = 0.3$. One dataset will consist of $(H(z), z)$ without noise while the second dataset will contain 10% Gaussian noise on $H(z)$ to see how big an impact noise has on the performance of the algorithms. For each dataset we compute 1000 data points distributed equidistantly in the redshift interval $z \in [0.1, 2]$, roughly representing the redshift interval of real datasets that directly measure the Hubble parameter (e.g. cosmic chronometers [19–22]).

We will additionally consider a dataset that corresponds to several Λ CDM models where we let H_0 and $\Omega_{m,0}$ vary in the intervals $H_0 \in [20, 100]$ in units of km/s/Mpc and $\Omega_{m,0} \in [0.1, 0.5]$. Again, we use equidistant points, now with 50 points for each feature. This dataset, as well as those discussed in the following subsections, are motivated by the ambition to decipher which symbolic regression methods are most suitable for discovering hitherto unknown observational relations. The more general an observational relation is, the more interesting it is. It is therefore desirable to reveal observational relations that are valid for not just a single Λ CDM model but rather for, say, *all* FLRW models or Λ CDM models. We therefore wish to test how well symbolic regression methods can describe data representing one or more families of cosmological models such as sub-families of FLRW models rather than just a single FLRW model. Since this type of dataset will be inherently more complicated than datasets based on only a single FLRW model², we will not add noise to these datasets.

2.2 Redshift drift in standard cosmology

One of the biggest mysteries in cosmology is the physical nature of dark energy i.e. the source of accelerated expansion of the Universe [23]. The apparent accelerated expansion of the universe has, however, never been measured directly. The observable *redshift drift* represents a possibility to remedy this. The redshift of a luminous astronomical object changes with time. This change has been dubbed the redshift drift. Redshift drift was first discussed in [24, 25] from 1962 but it was there assessed that the effect was too small to be measurable within a reasonable time frame. Due to technological advances, it is presently expected that the effect can be measured with e.g. the Square Kilometer Array (SKA) Observatory [26].

For FLRW models, the redshift drift, δz , can be written as

$$\delta z = \delta t_0[(1+z)H_0 - H(z)], \quad (2.2)$$

²Note for instance that it was in [5, 6] found that the symbolic regression algorithm AI Feynman [7, 8] was much better at finding analytical expressions for the redshift drift of a single cosmological model than for several models at once.

where $H(z)$ is the Hubble parameter, H_0 the Hubble constant and δt_0 is the time interval of the observation such that an object observed to have redshift z at time t_0 will be observed to have the redshift $z + \delta z$ at time $t_0 + \delta t_0$.

The expression for the redshift written above is fairly simple. Indeed, it represents only a small step in advancement from the direct Hubble data we considered in the previous section. Nonetheless, written as above, it represents an interesting symbolic regression problem because the right hand side of the equation contains a feature $H(z)$ which depends on the other feature (z) in a non-trivial way. In addition, $H(z)$ depends on the cosmological model parameters such as $\Omega_{m,0}$ which is not included as a parameter in the dataset since z and $H(z)$ are enough to obtain the expression for the redshift drift shown above. Earlier studies into machine and deep learning algorithms have included datasets where two or more variables were dependent, but these dependencies are typically linear or otherwise simple (see e.g. [27] for an example). However, to the authors' knowledge, there have not been conducted systematic studies of the impact of the interdependency of features nor studies based on datasets where features have more complicated dependencies such as in the case of the Hubble parameter and its dependence on the redshift.

In cosmology, observable relations are often more convenient to consider in terms of several dependent features. Besides the redshift drift, this is for instance the case for redshift-distance relations which are usually written as an integral over the Hubble parameter in terms of the redshift multiplied by factors containing the redshift itself as well. In our benchmark dataset we will therefore include the redshift drift as written above, i.e. with the target being $\delta z/\delta t_0$ and the features being z and $H(z)$. However, we will consider only flat, single-component FLRW models when generating the datasets. In this case, a simple rewriting gives that the redshift drift can be written as

$$\delta z = \delta t_0 H_0 [(1+z) - (1+z)^{3(1+\omega)/2}], \quad (2.3)$$

where ω is the equation-of-state parameter of the single component of the content of the model universe³.

Using the formalism discussed above, we have generated two redshift drift datasets, $(\delta z/\delta t_0, z, H(z))$ and $(\delta z/\delta t_0, z, \omega)$. The two models contain the same number of features, has the same target and contains the same number of data points generated using 50 equidistant points in each of the two intervals $z \in [0.1, 1]$ and $\omega \in [-0.99, 1/3]$. When choosing the redshift interval, we deliberately avoid the very lowest redshifts to avoid a target very close to zero. We choose the upper limit $z = 1$ since this is the upper limit expected for main redshift drift measurements from SKA [26]. For ω we choose the upper limit of $1/3$ which corresponds to the equation-of-state parameter for radiation while we choose a lower limit close to that of a cosmological constant, although neglecting the value -1 to keep the overall form of the Hubble parameter the same for all models⁴.

2.3 Cosmic backreaction and two-region models

The expression for the redshift drift given in the previous section is valid only for FLRW spacetimes, i.e. in spacetimes which have no structures on any scales. Standard cosmology is

³We could equally well have written out the Hubble parameter in terms of $\Omega_{m,0}$, z , and H_0 as when we considered the Hubble parameter but since the difference between the targets in the datasets with the Hubble parameter versus the redshift drift would very small, we expect the symbolic regression algorithms would perform similarly to as on the Hubble datasets.

⁴Remember that for flat, single component universes, $H(z) = \frac{2}{3(1+\omega)t}$ except for the case $\omega = -1$ where the Hubble parameter is constant.

based on the assumption that the large-scale dynamics of the Universe can be approximated well by the FLRW models but it has also been discussed whether the structures on smaller scales can affect the large-scale/averaged dynamics. This possibility is known as cosmic backreaction [28–31] and it has even been suggested that the seemingly accelerated expansion of the Universe is an artifact due to this phenomenon (the co-called backreaction conjecture – see e.g. [32–35]). Backreaction and the backreaction conjecture are most commonly considered through the Buchert equations presented in [36–38] where dynamical equations describing the average (large-scale) evolution of the Universe are obtained by averaging Raychaudhuri’s equation and the Hamiltonian constraint using the averaging definition

$$s_D := \frac{\int_D s dV}{\int_D dV}, \quad (2.4)$$

where s is some scalar and dV is the proper infinitesimal volume element on the spatial domain D assumed to be larger than the homogeneity scale. This definition can be used when considering spacetimes foliated with spatial hypersurfaces orthogonal to the fluid flow (possible for irrotational fluids such as dust) and where the line element is written as

$$ds^2 = -dt^2 + g_{ij} dx^i dx^j. \quad (2.5)$$

The resulting averaged Hamiltonian constraint and Raychaudhuri equation can be written as (setting $c = 1$)

$$\begin{aligned} 3H_D^2 &= 8\pi G\rho_D - \frac{1}{2}R_D - \frac{1}{2}Q_D \\ 3\frac{\ddot{a}_D}{a_D} &= -4\pi G\rho_D + Q_D. \end{aligned} \quad (2.6)$$

$H_D := \dot{a}_D/a_D$ denotes the average Hubble parameter and is related to the local fluid expansion scalar θ by $H_D = \theta_D/3$ (dots denote derivative with respect to time). The volume/averaged scale factor a_D is, unlike the scale factor in FLRW spacetimes, not related to the metric (which is not considered in the Buchert averaging scheme) but is instead defined as $a_D := (V_D/V_{D_0})^{1/3}$, where V_D is the proper volume of the spatial domain D and subscripts zero indicate evaluation at present time.

The dynamical equations for the average universe shown above are reminiscent of the Friedmann equation and acceleration equation but contain an extra term, namely $Q_D := 2/3 [(\theta^2)_D - (\theta_D^2)] - (\sigma_{\mu\nu}\sigma^{\mu\nu})_D$, where $\sigma_{\mu\nu}$ is the shear tensor of the fluid. In addition, the curvature term R_D can deviate from the FLRW behavior where the curvature must be proportional to the inverse of the squared scale factor. Q_D is sometimes referred to as the kinematical backreaction while the deviation of R_D from having FLRW evolution is referred to as intrinsic backreaction. Combined, these two differences with respect to the FLRW models mean that the large-scale dynamics of an inhomogeneous universe does not necessarily follow FLRW dynamics even when averaging above the homogeneity scale.

The two backreaction terms are coupled through the integrability condition

$$a_D^{-6}\partial_t(a_D^6 Q_D) + a_D^{-2}\partial_t(a_D^2 R_D) = 0. \quad (2.7)$$

This equation ensures that the two Buchert equations are consistent with each other. However, the two Buchert equations and the integrability condition do not form a closed set so cannot be used to predict backreaction, not even qualitatively. Therefore, it is unknown how

backreaction is realistically parameterized in terms of the scale factor (or equivalently, the mean redshift $\langle z \rangle + 1 \approx 1/a_D$ [39, 40], where triangular brackets indicate taking the mean over many lines of sight to remove statistical fluctuations). As discussed in e.g. [5, 6], this means that backreaction cannot be sensibly constrained with current cosmological data. This motivated an attempt (presented in [5, 6]) to obtain parameterizations for backreaction using toy cosmological models where backreaction can be computed, combined with symbolic regression to identify symbolic expression for backreaction. Building on that study, our benchmark dataset includes several datasets based on the so-called two-region models introduced in [41, 42].

Two-region models are toy cosmological models consisting of an ensemble of two different FLRW regions. Since the ensemble is disjoint, the model is not an exact solution to Einstein's equation. The model is nonetheless convenient to use for studying backreaction because the model is numerically fast and simple to work with. Following the procedure in [41, 42] we will consider a two-region model where one model is the empty (Milne) solution while the other region is an overdense (density larger than the critical density) matter+curvature model. In this case, the scale factors, a_o and a_u , of the two regions can be related by a common time coordinate, t , by using a parameter, ϕ (sometimes denoted the development angle), according to

$$\begin{aligned} t &= t_0 \frac{\phi - \sin(\phi)}{\phi_0 - \sin(\phi_0)} \\ a_u &= \frac{f_u^{1/3}}{\pi} (\phi - \sin(\phi)) \\ a_o &= \frac{f_o^{1/3}}{\pi} (1 - \cos(\phi)). \end{aligned} \tag{2.8}$$

The parameters f_u and f_o denote the present-time relative volume fractions of the two regions in the ensemble and are related by $f_u = 1 - f_o$. As in [41, 42], present time is defined to correspond to $\phi_0 = 3/2\pi$. As noted in e.g. [6], once f_u or f_o has been fixed, there is still one parameter which needs to be set in order to specify a two-region model uniquely. This is seen by noting that $H_D = H_u(1 - v + vh)$, where v is the time dependent volume fraction of the overdense region and $h := H_o/H_u$. Since $H_u = 1/t$ we therefore have $t_0 = (1 - v_0 + v_0 h_0)/H_{D_0}$ and thus need to fix either t_0 or H_{D_0} . We set $H_{D_0} = 70\text{km/s/Mpc}$.

Since both Q_D and R_D have unknown parameterizations in terms of a_D , we have used two types of two-region datasets for the benchmark, namely with Q_D and R_D as target, respectively. We first consider only a single two-region model specified by $f_o = 0.2$, yielding the datasets $(Q_D, \langle z \rangle)$ and $(R, \langle z \rangle)$. We then vary f_o as well as z , leading to the datasets $(Q, \langle z \rangle, f_o)$ and $(R_D, \langle z \rangle, f_o)$. Since f_o cannot easily be related to FLRW-quantities and hence quantities we often seek to constrain through observations, we also consider the datasets $(Q_D, \langle z \rangle, \Omega_{m,0}, \Omega_{R,0}, \Omega_{Q,0}, H_{D_0})$ and $(R_D, \langle z \rangle, \Omega_{m,0}, \Omega_{R,0}, \Omega_{Q,0}, H_{D_0})$, where we have defined

$$\begin{aligned} \Omega_{m,0} &:= 8\pi/(3H_{D_0}^2)\rho_{D,0} \\ \Omega_{R,0} &:= -R_{D,0}/(6H_{D_0}^2) \\ \Omega_{Q,0} &:= -Q_{D,0}/(6H_{D_0}^2). \end{aligned} \tag{2.9}$$

Based on the findings in [5, 6], the data points were generated using equidistant points in the intervals $\langle z \rangle \in [0.1, 1]$ and $f_o \in [0.1, 0.25]$.

Since the ground truths of the symbolic expressions for Q_D and R_D in terms of the features in these datasets are unknown, we assess the success of the symbolic regression algorithms by 1) evaluating their precision on the training model subspace using the mean squared error (MSE), and 2) evaluating their precision on data generated outside the model subspace used for training. Specifically, if a symbolic expression reproduced the data well within the training region, we also considered its performance on a test dataset corresponding to models in the larger interval $z \in [0, 5]$ and $f_o \in [0.05, 0.3]$. The reasoning here is that if a symbolic expression represents the ground truth, it must also be able to reproduce data outside the region it was trained on.

As detailed in [41, 42], the averaged deceleration parameter q_D can be written as

$$\begin{aligned} q_D &:= -\frac{1}{H_D^2} \frac{\ddot{a}_D}{a_D} = q_u \frac{1-v}{(1-v+hv)^2} + q_o \frac{vh^2}{(1-v+hv)^2} - 2 \frac{v(1-v)(1-h)^2}{(1-v+hv)^2} \\ &= q_o \frac{vh^2}{(1-v+hv)^2} - 2 \frac{v(1-v)(1-h)^2}{(1-v+hv)^2}, \end{aligned} \quad (2.10)$$

where to reach the second line we simply use that the empty region is coasting and hence $q_u = 0$. The last term is the backreaction term due to Q_D . By comparing with the Equations 2.6 we see that we can write Q_D as e.g.

$$\begin{aligned} Q_D &= 6H_D^2 \frac{v(1-v)(1-h)^2}{(1-v+hv)^2} \\ &= -6 \left(\frac{\ddot{a}_D}{a_D} + \frac{1}{2a_D^3} H_{D_0}^2 \Omega_{m,0} \right). \end{aligned} \quad (2.11)$$

The above two expressions are fairly straightforward analytical expressions. However, both expressions contain several dependent variables since v, h, H_D, \ddot{a}_D and a_D all depend on time (differently) which may make the regression task more complicated. We will therefore include (Q_D, H_D, v, h) and $(Q_D, H_{D_0}, \Omega_{m,0}, a_D, \ddot{a}_D)$ as datasets used for our benchmark to complement the earlier datasets for the target Q_D where there is no known ground truth expression.

2.3.1 Redshift drift in 2-region models

The redshift drift is a particularly interesting observable in relation to backreaction and the backreaction conjecture because it can be used as a smoking gun signal for distinguishing between accelerated expansion due to dark energy versus apparent acceleration due to backreaction [43–46]. The foundation for the smoking gun signal is that the mean redshift drift is not in general equal to the drift of the mean redshift in an inhomogeneous spacetime even if that spacetime is statistically homogeneous (where “mean” observations here indicate observations after taking the mean over many lines of sight in order to remove statistical fluctuations). Mathematically, we can write this statement as

$$\langle \delta z \rangle \neq \delta \langle z \rangle = \delta t_0 [(1 + \langle z \rangle) H_{D,0} - H_D(\langle z \rangle)], \quad (2.12)$$

where we set $\langle z \rangle + 1 = 1/a_D$. As discussed in [5, 6], an expression for $\langle \delta z \rangle$ in inhomogeneous cosmological models exhibiting backreaction is unknown. The redshift drift can nonetheless be computed in concrete cosmological models exhibiting backreaction as was done in [43, 44], with the former utilizing two-region models.

The procedure for computing the redshift drift in two-region models is to arrange copies of the two FLRW regions consecutively after one another along a light ray propagated according to the equations

$$\frac{dt}{dr} = -a \quad (2.13)$$

$$\frac{dz}{dr} = (1+z)\dot{a} \quad (2.14)$$

$$\frac{d\delta z}{dr} = \dot{a}\delta z + (1+z)\ddot{a}\delta t \quad (2.15)$$

$$\frac{d\delta t}{dr} = -\dot{a}\delta t, \quad (2.16)$$

where the scale factor is evaluated according to which local FLRW model it is in at any given position along the light ray. The redshift z is the local redshift along a light ray which approximates $\langle z \rangle$ as discussed in [43]. The resulting z and δz data only approximates their mean counterparts as they do contain small statistical fluctuations which means that these datasets have a small statistical error applied to them.

By solving the above equations, we generate datasets of the form $(\langle \delta z \rangle / \delta t_0, \langle z \rangle, \Omega_{m,0}, \Omega_{R,0}, \Omega_{Q,0})$, $(\langle \delta z \rangle / \delta t_0, \langle z \rangle, H_D(\langle z \rangle), \Omega_{m,0}, \Omega_{R,0}, \Omega_{Q,0})$ and $(\langle \delta z \rangle - \delta \langle z \rangle / \delta t_0, \langle z \rangle, \Omega_{m,0}, \Omega_{R,0}, \Omega_{Q,0})$, where the two latter datasets are inspired by the fact that we know that the symbolic expression for the FLRW redshift drift requires either an equation of state parameter or Hubble parameter. The datasets were generated using 50 equidistant points of $f_o \in [0.1, 0.25]$ and approximately 200 values of the redshift in the interval $z \in [0.1, 1]$.

As with the earlier two-region model datasets, we will assess the quality of the symbolic expressions obtained by the regression algorithms by seeing how well they generalized outside the model subspace the algorithms were trained on. Specifically, we make test datasets with the feature intervals $z \in [0.1, 5]$ and $f_o \in [0.01, 0.3]$.

2.4 Summary of data sets

Our cosmological datasets used for the benchmark are summarized in Table 1. Note that some targets are scaled to be of the order 1-10 in order to improve the symbolic regression. The feature intervals indicated in the table are for training data only. For datasets with unknown ground truth we assess the output from the symbolic regressions algorithms by comparing with a test dataset where the feature intervals are broadened. If the obtained symbolic expressions signify (the hitherto unknown) ground truths, they must perform well not only within the training interval but also in the test data representing the broadened parameter spaces. Otherwise, a symbolic expression with small MSE on the training data will simply represent a good (over-)fit without any (clear) physically relevant information. For the test data without known ground truths we use $z \in [0.1, 5]$ and $f_o \in [0.01, 0.3]$ to test the symbolic expressions outside the training regions.

Several datasets correspond to the same data but where different features are provided in the datasets. For some datasets, e.g. *C5* and *C6*, this is because features used for parametrizing targets in cosmology are often inter-dependent. We wish to see how such inter-dependence affects the regression algorithms' ability to find the ground truth expressions. Therefore we parameterize the same datasets using different parameters with some datasets having

inter-dependent features and some datasets having strictly independent features. For other datasets, we use different parameterizations because the underlying ground truth is not known. We therefore do not know exactly which features the symbolic regression algorithms will benefit from knowing. For all the datasets based on two-region models we additionally note that the models are parameterized by a single parameter f_o which is, however, not useful for obtaining general expressions for the targets valid also for cosmological settings not based on two-region models. Datasets based on two-region models are therefore considered both with f_o as a feature and with more cosmologically generic features such as density parameters.

Dataset name	Dataset	Data interval	Error
C1	$(H z)$	$z \in [0.1, 2], N = 1000$	\times
C2	$(H z)$	$z \in [0.1, 2], N = 1000$	10%
C3	$(H z, \Omega_{m,0})$	$z \in [0.1, 2], \Omega_{m,0} \in [0.1, 0.5], N = 100$	\times
C4	$(H z, H_0, \Omega_{m,0})$	$z \in [0.1, 2], \Omega_{m,0} \in [0.1, 0.5], h \in [20, 100], N = 50$	\times
C5	$(\delta z / \delta t_0 z, H(z, \omega))$	$z \in [0.1, 2], \omega \in [-0.99, 1/3], N = 100$	\times
C6	$(\delta z / \delta t_0 z, \omega)$	$z \in [0.1, 2], \omega \in [-0.99, 1/3], N = 100$	\times
C7	$(10^2 \cdot Q_D z)$	$z \in [0.1, 1], N = 1000$	\times
C8	$(10^8 \cdot R_D z)$	$z \in [0.1, 1], N = 1000$	\times
C9	$(10^2 \cdot Q_D z, f_o)$	$z \in [0.1, 1], f_o \in [0.1, 0.25], N = 50$	\times
C10	$(10^8 \cdot R_D z, f_o)$	$z \in [0.1, 1], f_o \in [0.1, 0.25], N = 50$	\times
C11	$(10^2 \cdot Q_D z, \Omega_{m,0}, \Omega_{R,0}, \Omega_{Q,0}, H_{D_0})$	$z \in [0.1, 1], f_o \in [0.1, 0.25], N = 50$	\times
C12	$(10^8 \cdot R_D z, \Omega_{m,0}, \Omega_{R,0}, \Omega_{Q,0}, H_{D_0})$	$z \in [0.1, 1], f_o \in [0.1, 0.25], N = 50$	\times
C13	$(10^2 \cdot Q_D H_D, v, h)$	$z \in [0.1, 1], f_o \in [0.1, 0.25], N = 50$	\times
C14	$(10^2 \cdot Q_D H_{D_0}, \Omega_{m,0}, a_D, \ddot{a}_D)$	$z \in [0.1, 1], f_o \in [0.1, 0.25], N = 50$	\times
C15	$(10^3 \cdot \langle \delta z \rangle / \delta t_0 z)$	$z \in [0.1, 1], f_o \in [0.1, 0.25], N = 50$	(\times)
C16	$(10^3 \cdot \langle \delta z \rangle / \delta t_0 z, f_o)$	$z \in [0.1, 1], f_o \in [0.1, 0.25], N = 50$	(\times)
C17	$(10^3 \cdot \langle \delta z \rangle / \delta t_0 z, \Omega_{m,0}, \Omega_{R,0}, \Omega_{Q,0})$	$z \in [0.1, 1], f_o \in [0.1, 0.25], N = 50$	(\times)
C18	$(10^3 \cdot \langle \delta z \rangle / \delta t_0 z, H_D, \Omega_{m,0}, \Omega_{R,0}, \Omega_{Q,0})$	$z \in [0.1, 1], f_o \in [0.1, 0.25], N = 50$	(\times)
C19	$(10^2 \cdot (\langle \delta z \rangle - \delta(z)) / \delta t_0 z, \Omega_{m,0}, \Omega_{R,0}, \Omega_{Q,0})$	$z \in [0.1, 1], f_o \in [0.1, 0.25], N = 50$	(\times)

Table 1. Summary of cosmological datasets used in the benchmark. In the rightmost column we indicate whether the given dataset has been attributed a Gaussian distributed 10 % error or no error (indicated by an \times). The datasets based on redshift drift in two-region models have an un-quantified minor error which we indicate by (\times) . N indicates the number of equidistant points along each feature dimension. For the two-region redshift drift data, the data points are not exactly equidistant along the z -dimension. In addition, N for the z -interval in these datasets are approximately 200 while the N indicated in the table is for f_o only. Datasets are indicated as (target|features).

3 Benchmarking with cosmological datasets

We bench the symbolic regression algorithms/models listed in Table 2. We assembled this collection of algorithms based on the availability of algorithms and a wish to consider algorithms based on a variety of methods. Additionally, we consider only algorithms that are generic in terms of the dataset types and thus do not consider algorithms which are specifically designed for, say, regression on redshift-distance data. Each model (except FFX) has several hyperparameters and other features which can be tuned. As described below, we have tuned the hyperparameters using a set of seven standard datasets with one to three features each. These datasets were chosen among standard datasets used for tuning hyperparameters of symbolic regression algorithms and are listed in Appendix A [59]. Tuning hyperparameters on a generic test dataset is a simple way of avoiding biasing for/against any of the algorithms or datasets in the tuning. We simply tune using standard datasets used in the symbolic regression community and which have no relation to cosmological datasets (see Subsection 3.1.3 for more details on the hyperparameter tuning). The tuned hyperparameters can be

Algorithm List				
Algorithm Name	Ref	Method	Multi-core	Year
AI-Feynman	[47, 48]	PI,NN	No	2020
Deep Symbolic Optimization (DSO)	[49, 50]	RNN,RL	Yes	2021
Deep Symbolic Regression (DSR)	[51]	RNN,RL,GP	Yes	2021
Fast Function Extraction (FFX)	[52]	GP	Yes	2011
Genetic Engine	[53]	GP	No	2022
GPZGD	[54]	GP	Yes	2020
ITEA	[55]	GP	Yes	2019
PySR	[56]	GP,NN	Yes	2023
QLattice Clinical Omics (QLattice)	[57]	GP	Yes	2022
Unified Deep Symbolic Regression (uDSR)	[49, 58]	RNN,RL	Yes	2022

Table 2. Algorithms considered in this paper including the ML methods they use, if they support multi-core in the current implementation and the year of release. We denote Physics Inspired as PI, Neural Network as NN, Recurrent Neural Network as RNN, Reinforcement Learning as RL, and Genetic Programming as GP. AI-Feynman predominantly runs single-core. DSO and uDSR are not using GP methods due to a limitation of the current implementation.

found in the publicly available code where all the algorithms are in the `methods` folder and hyperparameters are set in `procedure.py` (see Figure 1 for details). Note that the algorithms DSO and uDSR in principle support Genetic Programming (GP) methods but the interface we use currently using does not support this feature.

Regarding the algorithms we note that DSR and uDSR are further developments of DSO. From the test dataset we find that these algorithms are in some cases indeed able to find the correct expression. FFX is fast, has no hyperparameters and would only be able to provide the correct symbolic equation in very limited cases. GPZGD and Genetic Engine were hard to tune and the former did not recover any of our test equations. AI-Feynman is rather slow, but was able to find one equation. Of the purely genetic algorithms QLattice and ITEA perform the best. PySR is also one of the more successful algorithms according to the training done on the test datasets.

The authors of this paper are aware of the existence of the benchmark tool SRBench [60] and have used it as inspiration. Due to e.g. technical issues, we found it easier to make a new tool, and create our own documentation. The main guide for designing the tool has been to make it as user-friendly as possible both in terms of implementation and adding extensions.

3.1 Benchmarking method

In this section we discuss the benchmark tools developed for this paper and the procedure we have used to achieve the results presented in Section 3.2.

3.1.1 Framework

As part of this paper we release the code `cp3-bench` and `Things-to-bench` used for the benchmarking presented in this paper. The release contains two components. Firstly, we are releasing the benchmark engine which we call `cosmology` and `particle physics phenomena benchmark` (`cp3-bench`). Secondly, we release our `Things-to-bench` wrapper repository showcasing how one can leverage the benchmark tool in an easy way, and create a simple script to loop over datasets of interest. The latter repository contains the datasets used here, the

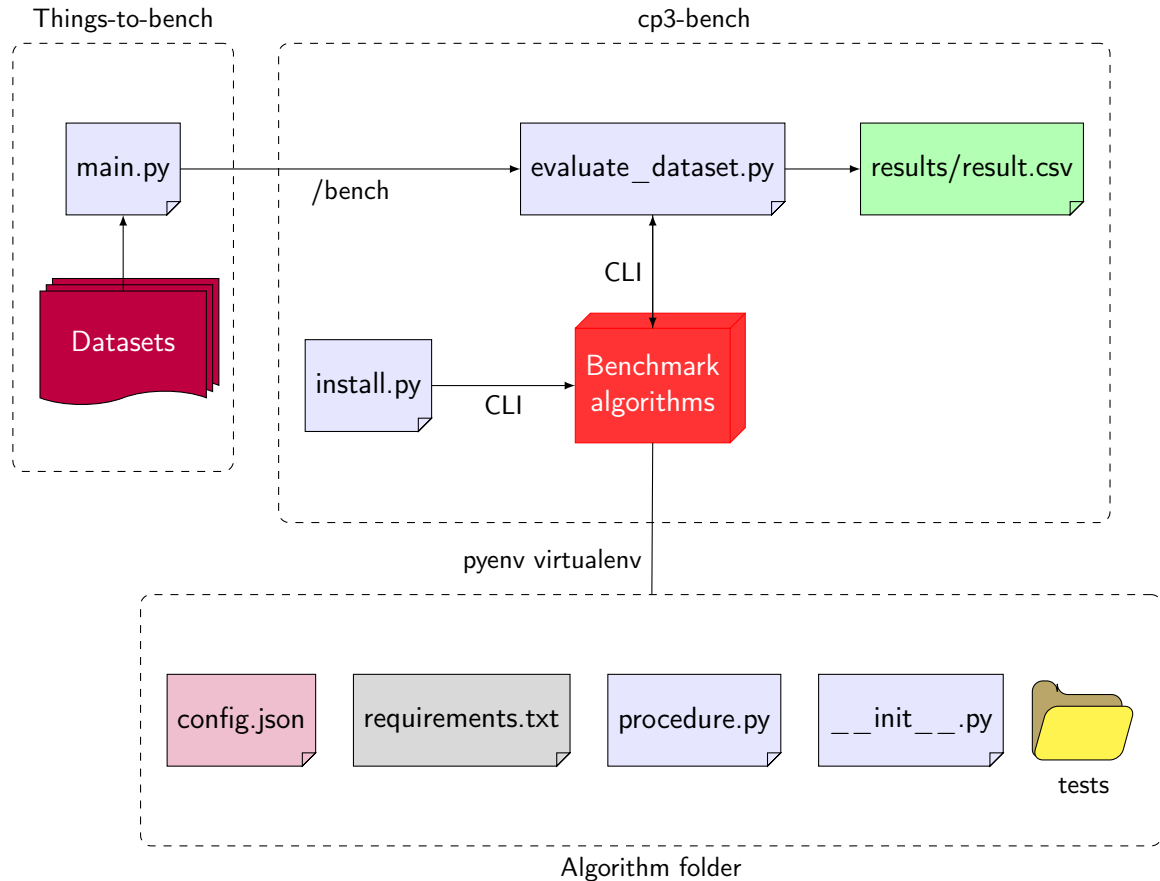


Figure 1. Architecture diagram showcasing the interaction between Things-to-bench and cp3-bench. The diagram contains an exploded view of the algorithm folder structure running in a pyenv virtual environment.

code used to run them, as well as the raw results including mathematica notebooks used to simplify and prepare the data for presentation in Appendix B. The code can be found at:

- cp3-bench (v1.0.0): <https://github.com/CP3-Origins/cp3-bench>
- Things-to-bench: <https://github.com/CP3-Origins/Things-to-bench>

Things-to-bench represents an example of interacting with the benchmark engine, cp3-bench, and it is used for inputting datasets of interest into the benchmark engine as shown in Figure 1. In this example, the interaction consists of importing the `evaluate_dataset.py` module found in the `bench` folder of cp3-bench. This is the main module for benchmarking.

We release cp3-bench with ten algorithms implemented and readily available for use. Adding new algorithms is straightforward by creating a new folder in the `methods` folder with the structure described in Figure 1. The program uses the folders in `methods` to recognize which methods are implemented. The default is to install all models when running the module `install.py`. Both modules can be imported to other scripts or run with CLI (command-line interface) and has the optional flag `--methods` which allows the user to select specific algorithms to install or benchmark. The install module also allows for the optional flag `--reinstall` which by default is false, but can be chosen to be true to reinstall a misbehaving

algorithm. The module `evaluate_dataset.py` requires an argument specifying the path to a `.csv` dataset to evaluate. This flag is called `--data_path`.

Each algorithm runs in a `pyenv` virtual environment allowing each algorithms to run a specific version of python with packages and dependencies installed specifically to the needs of the given algorithm.

The `tests` folder contains the configuration of universal tests, which each algorithm should pass. During installation these are used to verify the functioning of the algorithms.

In the `requirements.txt` file, Python dependencies of the package are specified. The `config.json` file contains the name of the algorithm, the key, which must match the folder name of the algorithm, the python version to use for creating the virtual environment with `pyenv`, and install commands which specifies any additional steps to perform in order to install the algorithm.

The most important file is the `procedure.py` script. Here the algorithm is imported and defined according to the framework. It is also where the hyperparameters are set. The script defines a class which initializes the algorithm and defines a procedure for training this algorithm. Note that some algorithms have a `format_output` function to reformat the output equation. Some implementations may also drop coefficients that are small or set small numbers to zero and round numbers to fewer significant digits to produce a shorter equation that is easier to read. In some cases, this formatting turns the symbolic expression found by the algorithm into the ground truth. In such a case, the MSE reported will not be zero, even though the output is exactly correct since the MSE is based on the unformatted result which contained small (errornous) additional terms. Some of the methods `cp3-bench` import have similar features built into the algorithm, one example is `uDSR` which can drop coefficients smaller than a specified value.

The algorithm classes inherit elements from a global superclass called `MethodEvaluator`. Most importantly, this class manages some logging levels and the evaluate method that is run during benchmarks. Specifically, it is run by the CLI interface that is used by `cp3-bench` to interact between the algorithms and the `evaluate_dataset.py` module.

The files and folders marked in the “Algorithm folder” part in Figure 1 are required for all algorithms. The individual algorithm may contain more files or folders beyond this minimum content. Anything that is created during the installation is put into a `deps` folder which is also created during installation.

The results of running the benchmark is saved as `.csv` files in a folder called `results` which is created when running the `evaluate_dataset.py` module the first time.

3.1.2 Getting started

This section aims at getting the reader started on using `cp3-bench`. To use this package you need the following:

- Ubuntu 20.04 or newer
- Python 3.10 or newer
- `pyenv`

Since this package relies on `pyenv` to manage virtual environments, it is key that this dependency is correctly installed and initialized. Otherwise you can face a wide variety of issues as mentioned in the `README.md` file on the GitHub repository page.

With the package downloaded from the root folder, and with `pyenv` correctly setup you can install Python dependencies:

```
1 pip install -r requirements.txt
```

Next, you can install the packages you want. **Remember** to correctly initialize `pyenv` otherwise almost nothing will work (see the documentation and trouble shooting section on the Github page of `cp3-bench`). The default is to install all algorithms:

```
1 python bench/install.py
```

but you can optionally pass `--methods` to specify algorithms such as DSR, FFX, and ITEA as in the example here:

```
1 python bench/install.py --methods dsr,ffx,itea
```

The result of the installation will be logged in the `STATUS.md` file in the `bench` folder. You can verify that everything is installed correctly by checking this file. There are four columns to consider:

- **Config:** Checks the configuration is valid
- **Environment:** Checks the environment is correctly setup
- **Installation:** Checks for successful installation of installed components
- **Tests:** Checks that all tests pass successfully

If a column is marked `[x]` then this step passed while `[-]` means failure. Consider the `reinstall` flag to try to reinstall the failed installation attempt for a given algorithm.

To use the package you need to parse a `.csv` file with the output value column named “target”. You can find short example of how this looks in the `tests/utis` folder by looking at the `test_dataset.csv` file.

In the setup described in Figure 1 we import `evaluate_dataset.py` as a module through:

```
1 from python.bench.evaluate_dataset import evaluate_dataset
2 evaluate_dataset(data_path="<path_to_dataset>")
```

and then parse the input to it as a regular Python module in/out script in `Things-to bench`. Alternatively you can also use CLI to evaluate a dataset using the following command from the root folder of `cp3-bench`:

```
1 python bench/evaluate_dataset.py --data_path <path_to_dataset>
```

Another option is to specify which algorithms to use by setting the appropriate flag, as with the installation command. The output is in the `results` folder.

3.1.3 Benchmark procedure

The primary goal of this paper is to evaluate the performance of symbolic regression models on cosmological datasets. Many of the models we include in the benchmark were originally tested by their creators on artificial standard datasets without direct application to cosmology or astrophysics, often making the regression task much easier. Therefore, we begin by considering a small sample of standard datasets, which can be found in Appendix A.

We optimize the hyperparamters to perform well across these standard datasets. Since the algorithms use different ML methods, it is not straightforward to compare the models one-to-one. For instance, certain models may be slower than others, while some models do

not benefit from extra time, as they have reached a minimum. It is therefore not generally meaningful to aim for a similar runtime. Runtime is nonetheless one quantitative measure of the usefulness of the model and we will therefore include it when comparing the algorithms below.

The models are all-in-all evaluated using three parameters: The resultant symbolic expression, the mean squared error (MSE), and runtime of the model. We define the MSE as

$$MSE = \frac{1}{n} \sum_{i=1}^n (\hat{y}_i - y_i)^2, \quad (3.1)$$

where n is the number of values in the output vector y and the prediction vector y_i .

We can thereby recognize that an algorithm may be somewhat slow compared to others, but if the symbolic expression is correct, then this is generally more important than having the model completing faster. On the other hand, if two models are equally good or poor at obtaining the correct symbolic expression, then a comparison of run times becomes relevant for differentiating the algorithms. The MSE is simply a measure of the global fit of the symbolic expressions. If an algorithm obtains the correct symbolic equation, the MSE will vanish. For all other situations, the MSE can be considered a measure of how far the resultant symbolic expression is from producing a meaningful result and possible ground truth. But one should remember that a low MSE is not necessarily equal to being close to finding the ground truth since an inherently incorrect expression may be fine-tuned to fit the data well within the training region.

We categorize the correctness of the result in the following three ways:

- ✓: A check-mark is used when the algorithm produced the correct equation up to a few conditions:
 1. The resultant equation is equal to the expected, possibly written in a different way. Consider the example where the expected equation is,

$$f(x) = x^2 + 1 \quad (3.2)$$

but the algorithm resulted in,

$$f(x) = \frac{x^3 + x}{x}. \quad (3.3)$$

This expression is considered correct.

2. The coefficients of the result are correct to the first significant digits. Assuming the equation from above, we would accept the following as correct,

$$f(x) = \frac{1.1x^3 + x}{x}. \quad (3.4)$$

3. Numbers smaller than or of the order $\mathcal{O}(10^{-10})$ are set to 0. For example,

$$f(x) = x^2 - 10^{-10}x + 1 \rightarrow f(x) = x^2 + 1, \quad (3.5)$$

is considered correct.

Compute hardware	
Type	Specification
OS	Ubuntu 24.04
CPU	2x Intel(R) Xeon(R) Gold 6130 @ 2.1GHz
Total core count	32 Cores
Total thread count	64 Threads
GPU	Integrated Matrox G200eW3 Graphics
Memory	384 GB

Table 3. Specification of the hardware used for benchmarking.

- ✓(MSE): We give a check-mark but with the MSE in parenthesis to indicate that the algorithms derived the correct equation at least structurally, but there are larger deviations than for the correct case such as:

1. The coefficients are not correct to the first significant digit. In this category, the result must still contain all the correct terms but there may be an additional term with a significantly smaller coefficient in front. Continuing with Equation 3.2 as the correct function, we would in this category allow larger deviations of the coefficient:

$$f(x) = 2x^2 + 0.3. \quad (3.6)$$

2. Residual terms that are less significant than the main terms of the result are accepted. For instance,

$$f(x) = x^2 - 0.0001x + 1, \quad (3.7)$$

is considered correct. The expression

$$f(x) = x^2 - x + 1, \quad (3.8)$$

is, however, not accepted in this category since the coefficient of the extra term is of the same order as the correct terms and the extra term is no longer considered a residue.

- MSE: Any expression deviating from the ground truth in ways not described above are considered incorrect and we indicate the deviation in terms of the MSE.

After tuning the models on the standard dataset (the result can be seen in Table 7), we run the cosmological datasets on the models and evaluate the results. This means our fine-tuning is blind to the cosmological dataset and we have only seen the results from benchmarking the cosmological data after we have locked the hyperparameters. In this way one can test the meaningfulness of optimizing for standard datasets and how well the models perform on cosmological datasets. The hardware used is described in Table 3.

Out of the box, the method `evaluate_dataset.py` will run multiple algorithms parallel, which might lead to some fight over resources if CPU is overloaded, but overall it will speed up the procedure and yield results faster. For the testing we kept the code as it is out of the box, **but** for the benchmarking of the cosmological dataset we specifically run only one algorithm per dataset at a time. This can be done by modifying the code, or by simply selecting to only use one algorithm at a time, instead of the default which is to use all algorithms.

3.2 Benchmarking results: Cosmological datasets

In this subsection we present the results from benchmarking the algorithms on our 19 cosmological datasets.

Table 4 gives a summary of the regression task for each algorithm in terms of the resulting MSEs. More details can be found in Appendix B where we show the symbolic expressions found by each algorithm for each dataset with the raw data being available in the Things-to-bench repository. Table 5 summarizes the datasets, comparing the ground truths with the most accurate expressions found by the algorithms.

Before discussing the results, we provide some comments regarding the presented MSE values and their reported equations: The algorithms considered are created by other authors and can come with unique features, and thus they behave in different ways. Therefore, some algorithms allow you to define thresholds for dropping certain residue terms, and some do these simplification out of the box without user input. Therefore, different algorithms do certain simplifications including rounding numbers to some number of significant digits.

When we compute the MSEs presented in the forthcoming tables, we use the full symbolic expression found by the algorithm. We call this the reported MSE. As explained above, the full symbolic expression is sometimes not identical to the reported expression (the expression printed out by the algorithm). This is simply because the reported expression may, as noted above, have residue terms drops and presented with less significant digits in order to make the output equation more presentable.

As part of the result processing we have extracted the reported equations into mathematica notebooks where we have recomputed the MSE based on the reported equation. We find that due to the mentioned simplifications, the reported MSE does not always match the MSE computed from the reported equation. We emphasize that the MSE values reported in this paper are those coming from the full symbolic expression identified by the given algorithm. This is also the MSE which is provided by cp3-bench.

For most algorithms we do not find significant deviations between the MSE computed using the full expression and the reported expression. However, there are some exceptions worth mentioning. We first note that GPZGD consistently showed a significantly lower reported MSE compared to the MSE of the reported expression. This was also the case for FFX for the more complicated equations corresponding to the datasets *C4*, *C6*, *C7*, *C12*, *C13*, *C16*, and *C17*. We attribute this to the fact that FFX only outputs 3 significant digits in the output equation, but the underlying equation identified by the algorithm can have more significant digits. The resulting differences between the reported MSE and the MSE obtained from the reported expression deviate more for more complicated and long equations. We further note that Genetic Engine and AI-Feynman do not protect against producing imaginary numbers. The results obtained from Genetic Engine on dataset *C19* and from AI Feynman on dataset *C6* for instance contained imaginary parts. In these cases, only the real value is reported by the algorithm. Such situations can also lead to differences in the reported MSE and the MSE of the reported algorithm. We also note that the reported equation of Genetic Engine would yield division by zero errors for one or more parameters considered for the datasets *C6*, *C8*, *C15*, *C16* and *C17*. This division by zero would presumably not appear in the exact expressions obtained before rounding etc. In general, the reported MSE and the MSE based on the reported equation were for QLattice very close to each other. The exception is for *C11* where the reported equation produces an MSE that is orders of magnitude

Cosmological dataset results										
Dataset	Algorithm									
	AI-Feynman	DSO	DSR	FFX	Genetic Engine	GPZGD	ITEA	PySR	QLattice	uDSR
C1	10^{-8}	10^{-5}	10^{-5}	10^{-6}	10^{-6}	10^{-13}	10^{-14}	10^{-9}	10^{-10}	✓
C2	10^{-14}	10^{-14}	10^{-14}	10^{-14}	10^{-14}	10^{-14}	10^{-14}	10^{-14}	10^{-14}	10^{-14}
C3	10^{-6}	10^{-4}	10^{-4}	10^{-6}	10^{-5}	10^{-6}	10^{-9}	10^{-6}	10^{-9}	✓
C4	10^{-5}	10^{-6}	10^{-5}	10^{-5}	10^{-6}	10^{-5}	10^{-8}	10^{-6}	10^{-7}	✓
C5	✓	10^{-4}	10^{-4}	✓	10^{-5}	✓(10^{-31})	✓	✓	✓	✓
C6	10^{-3}	10^{-4}	10^{-4}	10^{-6}	10^{-5}	10^{-7}	10^{-7}	10^{-5}	✓	10^{-8}
C7	10^{-6}	10^{-4}	10^{-5}	10^{-4}	10^{-6}	10^{-10}	10^{-13}	10^{-7}	10^{-11}	10^{-13}
C8	10^{-4}	10^{-3}	10^{-4}	10^{-4}	10^{-4}	10^{-7}	10^{-10}	10^{-6}	10^{-9}	10^{-11}
C9	10^{-3}	10^{-3}	10^{-3}	10^{-4}	10^{-4}	10^{-5}	10^{-6}	10^{-3}	10^{-6}	10^{-7}
C10	10^{-3}	10^{-2}	10^{-2}	10^{-3}	10^{-3}	10^{-3}	10^{-5}	10^{-2}	10^{-5}	10^{-6}
C11	10^{-3}	10^{-3}	10^{-3}	10^{-4}	10^{-3}	10^{-4}	10^{-7}	10^{-3}	10^{-6}	10^{-3}
C12	10^{-4}	10^{-2}	10^{-3}	10^{-3}	10^{-2}	10^{-1}	10^{-6}	10^{-3}	10^{-6}	10^{-2}
C13	10^{-3}	10^{-2}	10^{-3}	10^{-4}	10^{-4}	10^{-3}	10^{-5}	10^{-4}	10^{-6}	10^{-2}
C14	10^{-4}	10^{-3}	10^{-3}	10^{-4}	10^{-4}	10^{-5}	10^{-2}	10^{-3}	10^{-6}	10^{-3}
C15	10	10	10	10	10	10	10	10	10	10
C16	1	10^{-1}	10^{-1}	10^{-1}	10^{-2}	10^{-2}	10^{-2}	10^{-2}	10^{-2}	10^{-2}
C17	10^{-1}	1	10^{-1}	10^{-1}	10^{-2}	10^{-2}	10^{-2}	10^{-2}	10^{-2}	1
C18	1	10^{-1}	10^{-1}	10^{-2}	10^{-2}	10^{-3}	10^{-3}	10^{-2}	10^{-3}	1
C19	10^{-3}	10^{-4}	10^{-3}	10^{-3}	10^{-4}	10^{-4}	10^{-4}	10^{-4}	10^{-4}	10^{-2}

Table 4. Result of evaluating the cosmological datasets across all algorithms.

worse than the reported MSE based on the exact expression. Therefore, we have put this value in red in Tables 4 and 5.

We now move on to discuss the results presented in Tables 4 and 5. As seen in Table 4, a single algorithm, uDSR, identified the correct formula for dataset *C1*. When a 10 % Gaussian error is added to the dataset (*C2*), the MSE becomes significantly worse for the algorithms and no algorithm finds the correct mathematical formula. As seen in Table 9, the MSE of the result from all algorithms were of the order 10^{-4} and the MSE of uDSR was thus only slightly better than that of the other algorithms. The algorithm uDSR also finds the correct expression for *C3* and *C4*, although this requires modest rewriting of the final results as written in Table 5 to see. For *C5* we note that both Qlattice, PySR, and uDSR find the correct formula up to at least 3 significant digits but that Qlattice has a somewhat smaller MSE, presumably due to the final digits. ITEA also nearly finds the correct formula, the error being one highly suppressed extra term which is order $\mathcal{O}(10^{-10})$, and thus we have dropped it in Table 12. The dropped term is retained in the raw data. AI-Feynman, FFX and GPZGD also find the correct form of the data, although with somewhat incorrect coefficients, and for GPZGD the difference is so big we classify it as only “almost correct” and note the MSE. Although *C5* and *C6* represent the same datasets, our benchmark shows that their different parameterizations are quite important; only Qlattice succeeds with finding the correct formula for *C6*. Thus, the simpler symbolic form of the dataset when represented by the dataset *C5* is quite important for the algorithms’ ability to identify the correct formula. This is particularly interesting because the parameters in *C5* are inter-dependent which could potentially have made it more difficult for the algorithms to identify the correct formula. Such inter-dependence of parameters thus appears to be much less important than the complexity of the formula. When we move on to the datasets *C13* and *C14* which represent the more complicated expressions, none of the algorithms come particularly close to the correct expression. We also note that the algorithms do not do note-worthily better on *C14* despite

Dataset name	Ground truth	Best result	MSE	Algorithm
C1	$H = 0.0716/\text{Gyr} \cdot \sqrt{0.3 \cdot (1+z)^3 + 0.7}$	$H = 0.0716 \cdot \sqrt{0.3 \cdot (1+z)^3 + 0.7}$	10^{-30}	uDSR
C2	$H = 0.0716/\text{Gyr} \cdot \sqrt{0.3 \cdot (1+z)^3 + 0.7} + \text{error}$	$0.932 + z(0.279 + z(-1.31 + z(2.61 + (-2.08 + 0.576z)z))) + \sin\left(\frac{e^{z+\cos(e^{\sin(z)})}}\right)$	10^{-4}	uDSR
C3	$H = 0.0716/\text{Gyr} \sqrt{\Omega_{m,0}(1+z)^3 + (1-\Omega_{m,0})}$	$H = \sqrt{0.0051 + z(0.015 + (0.015 + 0.0051z)z)\Omega_{m,0}}$	10^{-30}	uDSR
C4	$H = H_0 \sqrt{\Omega_{m,0}(1+z)^3 + (1-\Omega_{m,0})}$	$H = 1.732H_0 \sqrt{0.33 + z(1+z + 0.33z^2)\Omega_{m,0}}$	10^{-29}	uDSR
C5	$\delta z/\delta t_0 = [0.0716/\text{Gyr} \cdot (1+z) - H(z)]$	$\delta z/\delta t_0 = 0.0716 - H + 0.0716z$	10^{-30}	QLattice
C6	$\delta z/\delta t_0 = 0.0716/\text{Gyr}[(1+z) - (1+z)^{3(1+\omega)/2}]$	$\delta z/\delta t_0 = 0.0716 + 0.0716z - 0.07159(1+z)^{1.5+1.5\omega}$	10^{-16}	QLattice
C7	unknown	$10^2 Q_D = \left((0.51 + z(2.2 + z(11 + z(9.9 + (32 - 4.6z)z))) \cos(\sin(z + \cos(z))) \right)^{1/4}$	10^{-13}	uDSR
C8	unknown	$10^8 R_D = \frac{7.2424e^{-z} \cos(z - \cos(z))}{-0.81024 + z(-3.2 + z(-3.6 + z(-2.1 + z(1.5 + z)))}$	10^{-11}	uDSR
C9	unknown	$10^2 Q_D = f_o(-f_o - \sqrt{z} + (18z)/f_o^4(-0.00080 - 0.0025z) - 0.00029f_o^2z^2 + f_o^3(-0.00032 + z(-0.0040 + 8.4z)) + f_o z(-7.5 + z(17 + z(-13 + 3.9z))) + z(5.9 + z(-10 + z(9.4 + z(-4.7 + z))))$	10^{-7}	uDSR
C10	unknown	$10^8 R_D = \frac{1}{f_o - \sqrt{\cos(\cos(z^2))}} \left(4.0 + f_o^4(-0.033 - 0.0048z) + f_o^3(-0.011 + (-0.0078 - 0.00045z)z) + f_o^2(-0.000026 + z(-0.0011 + (-0.00058 - 0.000042z)z)) + f_o(-7.30 + z^2(13 + z(-18 + 7.3z))) + z(-7.9 + z(11 + z(-11 + (7.2 - 2.3z)z))) \right)$	10^{-6}	uDSR
C11	unknown	$10^2 Q_D = 0.033 + 4.6 \tanh\left(0.29 \exp(-0.34z^2 + (-4.7 - 1.9\Omega_{Q,0})\Omega_{Q,0} + z(2.0 + 1.6\Omega_{Q,0}) - 0.39 \ln(0.33 + 8.7\Omega_{m,0}^2) \cdot (0.038 + \Omega_{m,0})^{1.2})\right)$	10^{-6}	QLattice
C12	unknown	$10^8 R_D = 64 - 4.7e^{\frac{H_0 \Omega_{Q,0} \Omega_{R,0}^3}{z^2 \Omega_{m,0}}} - 0.0048 \sqrt{\frac{z^5 \Omega_{Q,0}^3}{H_0^3 \Omega_{m,0}^2}} - 11 \cdot 10^4 \sqrt{\frac{H_0^5 \Omega_{Q,0}^5}{\Omega_{m,0}^5}} - 1.1 \ln\left(\frac{\Omega_{Q,0}^5 \Omega_{R,0}^5}{z^2 \Omega_{m,0}^4}\right) + 1.2 \sin\left(\frac{z^4 \Omega_{m,0}^3 \Omega_{R,0}^2}{\Omega_{Q,0}^2}\right)$	10^{-6}	ITEA
C13	$Q_D = 6H_D^2 \frac{v(1-v)(1-h)^2}{(1-v+hv)^2}$	$-0.015 + (9.3 - 4.3v)v + (0.0037 - 4.6v) \ln(e^{(1.7-0.76h)h+(4.5-50H)H})$	10^{-6}	QLattice
C14	$Q_D = -6 \left(\frac{\ddot{a}_D}{a_D} + \frac{1}{2a_D^3} H_D^2 \Omega_{m,0} \right)$	$10^2 Q_D = \exp(-0.00054e^{(2.8-3.7a_D)a_D}) \times (e^{27H}e^{-30H^2} + (-0.47 - 0.24\Omega_{m,0})\Omega_{m,0} + e^{(2.8-3.7a_D)a_D+(27-30H)H} \times (-0.052 - 0.053\Omega_{m,0})\Omega_{m,0} + e^{(5.6-7.4a_D)a_D+(53-61H)H} \times (-3.2 \cdot 10^{-7} + (-0.000061 - 0.0029\Omega_{m,0})\Omega_{m,0}))$	10^{-6}	QLattice
C15	unknown	$10^3 < \delta z > / \delta t_0 = 0.17 + (-11 - 14 \langle z \rangle) \langle z \rangle$	10	QLattice
C16	unknown	$f_o(\langle z \rangle^4 (0.000055 + 28f_o) + \langle z \rangle^3 (11 + f_o(-22 \cdot 10 + 53 \cdot 10f_o)) + \langle z \rangle^2 (-55 + f_o(0.00020 + (0.00010 - 19 \cdot 10^2 f_o)f_o)) + f_o^2(0.00041 + f_o(0.017 + (0.056 - 0.0013f_o)f_o)) + \langle z \rangle (-52 + f_o(-0.000091 + f_o(-78 \cdot 10 + (27 \cdot 10^2 - 34 \cdot 10^2 f_o)f_o))) + \cos(e^{f_o} + \cos(\langle z \rangle)))$	10^{-2}	uDSR
C17	unknown	$-21 \cdot 10 + \frac{15 - \frac{2.4 \langle z \rangle \Omega_{m,0}^2 \Omega_{R,0}^2}{\Omega_{Q,0}^2}}{H_D} + 68 \sqrt{\left \frac{\langle z \rangle^5 \Omega_{m,0}^5 \Omega_{Q,0}^2}{H_D \Omega_{R,0}^3} \right } - 23 \cdot 10^3 \sqrt{\left \langle z \rangle^2 H_D^3 \Omega_{m,0}^4 \Omega_{Q,0}^4 \Omega_{R,0}^5 \right } + 22 \sin\left(\frac{\langle z \rangle^2 \Omega_{m,0}^4 \Omega_{R,0}^5}{\Omega_{Q,0}^3}\right)$	10^{-2}	ITEA
C18	unknown	$-21 \cdot 10 + \frac{15 - \frac{2.4 \langle z \rangle \Omega_{m,0}^2 \Omega_{R,0}^2}{\Omega_{Q,0}^2}}{H_D} + 68 \sqrt{\left \frac{\langle z \rangle^5 \Omega_{m,0}^5 \Omega_{Q,0}^2}{H_D \Omega_{R,0}^3} \right } - 23 \cdot 10^3 \sqrt{\left \langle z \rangle^2 H_D^3 \Omega_{m,0}^4 \Omega_{Q,0}^4 \Omega_{R,0}^5 \right } + 22 \sin\left(\frac{\langle z \rangle^2 \Omega_{m,0}^4 \Omega_{R,0}^5}{\Omega_{Q,0}^3}\right)$	10^{-3}	ITEA
C19	unknown	$-4.8 + 6.2e^{z^2 \Omega_{Q,0} \Omega_{R,0}} - 1.4e^{\langle z \rangle^4 \Omega_{Q,0}^2 \Omega_{R,0}^5} - 12 \sqrt{\left \langle z \rangle^5 \Omega_{m,0}^5 \Omega_{Q,0}^2 \Omega_{R,0}^3 \right } - 1.1 \sqrt{\left \frac{\langle z \rangle \Omega_{Q,0}^5 \Omega_{R,0}^5}{\Omega_{m,0}^4} \right } - 4.3 \sin\left(\frac{\langle z \rangle \Omega_{m,0}^3}{\Omega_{Q,0}^2}\right)$	10^{-4}	ITEA

Table 5. Summary of best (smallest MSE or correct formula) symbolic expression found for each cosmological dataset. Ground truths are written with the target on the left hand side while any non-numeric on the right hand side represents a feature/parameter of the dataset. To increase readability we only include 2 or 3 significant digits. The MSE is only given to order of magnitude.

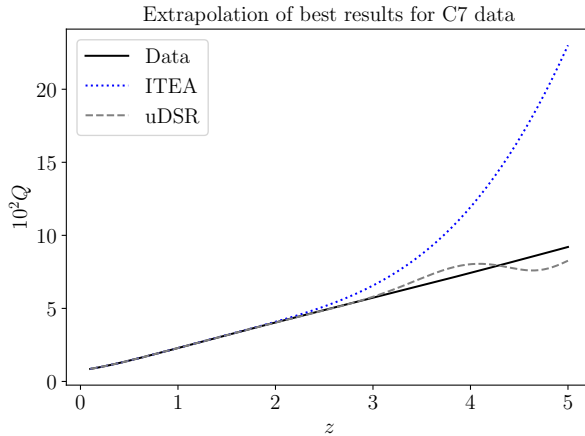


Figure 2. Comparison of correct data corresponding to dataset $C7$ extrapolated to $z = 5$ compared with best results from ITEA and uDSR. To ease readability of the graph, we only show lines corresponding to the single value of $f_o = 0.2$.

it representing a less complex expression⁵.

ITEA and uDSR have the lowest MSEs for the dataset $C7$. We therefore see how well the symbolic expressions found by these algorithms extrapolate into higher redshifts. In Figure 2 we show how well the expressions extrapolate to $z = 5$ for a specific value of f_o . It is quite clear from the comparison with the data that neither ITEA nor uDSR found a ground truth relation. We have made similar comparisons between the extended datasets with unknown ground truths with the best expressions found by each algorithm and note that although none of the algorithms find an expression that extrapolates well outside the training region, the expressions with the lowest MSE are often not the ones that extrapolate the best. For instance, AI Feynman and FFX both find symbolic expressions that extrapolate fairly well to $z = 5$ for the $C7$ data set. However, for $C7$, the symbolic expressions that extrapolate the best out to $z = 5$ are those found by Genetic Engine and QLattice which deviate at most 2% and 0.8%, respectively, from the data in the redshift interval $z \in [0, 5]$. Upon extrapolating up to $z = 10$ we find that the deviations increase up to over 10% and 8% (and are still growing linearly at this point). We therefore conclude that the expressions do not represent (approximate) ground truths, but that they may nonetheless be on the right track.

We lastly note that based on the ability to identify correct ground truths, uDSR overall performs the best of all the benched algorithms, identifying several of the ground truth expressions. We also note that for the cases where uDSR found the ground truth it was also incredible fast, in part thanks to its ability to stop early when the precision is deemed good enough. This algorithm did *not* perform noticeably better than the other algorithms on the test dataset (see Appendix A). Indeed, on the test data ITEA identified the correct formula for 4 of the datasets while uDSR, QLattice and PySR all identified the correct formula in only 3 instances. The remaining algorithms either identified one or zero correct symbolic expressions.

⁵Note that there are various ways to define the complexity of a function (see e.g. [61] for a summary). One of the more traditional methods is a simple count of number of operators, but often also the number of embeddings are evaluated. In both cases, the expression represented by $C14$ is simpler than that of $C13$.

4 Summary, discussion and conclusions

We have presented a benchmark of symbolic regression algorithms on cosmological datasets. Our results indicate that the algorithms that do the best on standardized datasets do not necessarily also perform best on cosmological datasets. For instance, we found that uDSR clearly did best on the cosmological datasets while performing only mediocre on the standardized data which had been used for hyperparameter tuning. This particular difference is likely due to the fact that the Hubble data, which uDSR performed well on, contains polynomial features which this algorithm is particularly optimized for. We also note that FFX failed to produce any correct equation for the standard datasets but did find one equation for the cosmological dataset.

Although we did not discover any new physical relations in the presented benchmark, we believe the framework of cp3-bench and our presented benchmark could help the community reach such goals in the future. In relation to this we note that to perform an unbiased benchmark, our hyperparameter tuning was done on standardized datasets and hence “blind” towards the cosmological datasets. This was also done since we wanted to see if the performance of the different algorithms on the standardized and cosmological datasets would be similar. It is possible that all (or some of) the algorithms could perform better on the cosmological datasets if hyperparameters had been tuned for each specific dataset. However, such a procedure is prone to leading to overfitting and could lead to biased results of the benchmark. We also note that relying solely on MSE inside the training region for evaluating the goodness of fit for an expression may not be prudent when seeking to identify hitherto unknown ground truths. We for instance notice that for some of our datasets, the expressions with the smallest MSEs quickly become wildly incorrect outside the training regions while several expressions with somewhat larger MSEs could be correct to around 1 % precision far outside the training region.

We considered the possibility that symbolic regression algorithms perform worse on datasets where features are inter-dependent as is often the case in cosmological datasets. However, we find no indication that this should be the case. Instead, we find that the symbolically simpler expression of dataset *C5* is identified by more algorithms than the expression corresponding to *C6*, even though the features of *C5* are inter-dependent while they are not so in *C6*. We further note that the symbolic regression task clearly depends on the precision of the training data. In particular, we find that a single algorithm can identify the correct expression for the exact data (no error) of *C1* while none identify it for the dataset *C2* where noise has been added, and the results based on *C2* are generally further from the ground truth than the results based on *C1*. We also note that the MSEs corresponding to *C2* are quite low for several of the algorithms despite the identified expressions being clearly incorrect. This is a reminder that symbolic regression can be prone to overfitting.

Our findings lead us to conclude that having a benchmark suite like cp3-bench, with algorithms using a rich variety of ML methods, can be a prudent part of the strategy, when aiming at discovering new physics with ML methods. We lastly note that our results overall indicate that there is still much room for enhancing the performance of symbolic regression algorithms. Based on our specific results, we identify possible paths for developers of symbolic regression algorithms. Firstly, one could consider methods for constraining the output using dimensional analysis. In principle, we do not need to consider dimensional analysis when doing symbolic regression since the pre-factors can be considered to implicitly contain any factors of e.g. c, G necessary for the dimensions of ones results to be correct. However, including

dimensional analysis in symbolic regression analysis has been discussed by others in e.g. [17] and might enhance the algorithms’ abilities in relation to physics data. To our knowledge, a systematic study of the impact of such analysis on modern astrophysics and particle physics data has not been conducted. By leveraging cp3-bench, such systematic studies become much simpler than if one must install all algorithms from scratch. Secondly, algorithms might be improved by carefully considering the choice of complexity allowed. Some algorithms like PySR have very good features for controlling the nesting, while others lack such features entirely, merely focusing on the number of terms. This can lead to rather unrealistic terms such as $e^{e^{\cos(x)}}$ which rarely appears in physics formulae. See e.g. [61] for further discussions of complexity measures. In addition, the algorithms (not surprisingly) in particular become inadequate when the feature space has dimension above ~ 2 . Thus, it could be useful if future development of symbolic regression algorithms for astrophysics purposes were focused e.g. on increasing performance of the algorithms on datasets with just a few more dimensions. Lastly, we note that, as also discussed in e.g. [62], ML algorithms are not generally aimed at the high precision required for identifying ground truth symbolic expressions. Methods aimed at increasing the precision of machine learning should therefore also be a focus when seeking to improve symbolic regression algorithms.

As a future improvement of cp3-bench one could develop an abstraction layer using the `format_output` function of the procedure class such that this would return the equation in a format compatible across the package, and then one could compute the MSE from the output equation of the algorithm and as an option output the MSE from the output equation and not the underlying full model. Alternatively, one could also do a check with this and warn the user if the two methods of computing the MSE are significantly diverging. Having this abstraction layer could also help control the output format of the equation to a standard and easier to use format. Currently, the output equation is largely shown as the underlying algorithm outputs it, which is not the same across the different algorithms.

Acknowledgments

We thank the authors of [10] and in particular Fabricio Olivetti de França and William La Cava for correspondence, and we thank H elo ise Delaporte for help with a mathematica script for converting symbolic expressions into easier readable formats.

SMK is funded by VILLUM FONDEN, grant VIL53032. Part of the numerical work done for this project was performed using the UCloud interactive HPC system managed by the eScience Center at the University of Southern Denmark.

Author contribution statement: MET wrote the benchmark code cp3-bench and Tings-to-bench based on a technical study of the presented algorithm and a literature study conducted by SMK. MET performed hyperparameter tuning with minor contributions from SMK who also contributed to installation tests. The considered datasets were produced by SMK. Both authors have contributed significantly to the writing of the manuscript and the development of the project.

A Standard datasets

The table below shows the dataset we have used to tune hyperparameters. The dataset is a combination of symbolic expressions found in standard datasets. The dataset and param-

eter/feature ranges were selected by considering the datasets listed in appendix A of [59], although parameter ranges were modified somewhat to improve the hyper parameter tuning.

Dataset name	Symbolic Expression	Parameter Interval
F1	$x^5 - 2x^3 + x$	$x \in [-10, 10], N = 1000$
F2	$0.3 \cdot x \sin(2\pi x)$	$x \in [-10, 10], N = 1000$
F3	$x^3 \cdot e^{-x} \cdot \cos(x) \cdot \sin(x) (\sin^2(x) \cos(x) - 1)$	$x \in [0, 10], N = 1000$
F4	$2.5x^4 - 1.3x^3 + 0.5y^2 - 1.7y$	$x, y \in [-3, 3], N = 100$
F5	$1.5e^2 + 5 \cos(y)$	$x, y \in [-3, 3], N = 100$
F6	$\frac{\exp(-(x-1)^2)}{1.2+(y-2.5)^2}$	$x, y \in [0.3, 4], N = 100$
F7	$0.23 + 14.2 \frac{x+y}{3z}$	$x, y, z \in [-5, 5], N = 30$
F8	$6.78 + 11\sqrt{7.23xyz}$	$x, y, z \in [0, 10], N = 30$

Table 6. Dataset of standard symbolic expressions used for hyperparameter tuning. The dataset is a small selection of the datasets listed in appendix A of [59]. The parameter intervals are indicated by giving upper and lower limit in the interval and the number (N) of equidistant points inside the interval. When expressions contain more than one parameter, the parameter intervals were identical for all parameters, with N indicating the number of data points in each dimension.

Test dataset results										
Dataset	Algorithm									
	AI-Feynman	DSO	DSR	FFX	Genetic Engine	GPZGD	ITEA	PySR	QLattice	uDSR
F1	10^1	✓	✓	10^6	✓	10^5	✓	✓	$\sqrt{(10^{-7})}$	✓
F2	10^{-1}	10^0	10^0	10^0	10^0	10^{-4}	10^0	10^0	10^0	10^0
F3	10^{12}	10^{11}	10^{10}	10^{11}	10^{11}	10^{10}	10^{12}	10^{10}	10^9	10^{10}
F4	10^2	10^1	10^1	10^1	10^1	10^0	✓	10^0	$\sqrt{(10^{-8})}$	✓
F5	10^{-2}	10^1	10^1	10^0	10^1	10^{-2}	✓	✓	10^{-9}	10^{-5}
F6	10^{-1}	10^{-2}	10^{-3}	10^{-5}	10^{-2}	10^{-3}	10^{-3}	10^{-3}	10^{-9}	10^{-7}
F7	✓	10^2	10^2	10^4	10^2	10^4	10^4	✓	$\sqrt{(10^{-6})}$	✓
F8	10^2	10^3	10^3	10^2	10^1	10^3	✓	10^3	10^2	10^2

Table 7. Result of the tuning of parameters on the test datasets.

Cosmological dataset: C1			
Algorithm	MSE	Equation	Runtime
AI-Feynman	$4.6203 \cdot 10^{-08}$	$0.070053 + 0.10276e^{\sqrt{e^{-z}}} z$	08:53:25
DSO	$7.6999 \cdot 10^{-05}$	$\sin\left(\sqrt{\frac{e^z}{z+e^5}}\right)$	01:26:47
DSR	$1.7932 \cdot 10^{-05}$	$\frac{z}{2\sqrt{z+4z+2}\sin(2z)}$	01:01:03
FFX	$1.7949 \cdot 10^{-06}$	$0.0719 + 0.0394z + 0.015z^2$	00:00:08
Genetic Engine	$3.0572 \cdot 10^{-06}$	$\frac{1}{-0.01+z}z \log\left(1 + \left 0.1 - \frac{0.0001}{z} - 0.0011z\right \right) \left(-0.001 + z(-0.000326228 + z(0.0226228 + z)) + (-0.01 + z)z\sqrt{\log\left(1 + \frac{0.1}{ z }\right)}\right)$	04:00:02
GPZGD	$3.0792 \cdot 10^{-13}$	$0.13409 - 0.0011566(211.91 + z(23.471 + z(3.8176 + z)))(\sin(0.018917 + 0.07528z) - \sin(\sin(0.24493z)))$	04:00:01
ITEA	$1.5824 \cdot 10^{-14}$	$0.0717424 - 7.29851 \cdot 10^{-6}e^{z^2} + 0.030679z^2 - 0.0042627 z ^{3/2} - 0.0001696 \cos(z^2) + 0.0332752 \sin(z)$	00:07:08
PySR	$2.1030 \cdot 10^{-9}$	$0.071640 + 0.028106z^2 + 0.031315 \sin(z)$	00:35:36
QLattice	$1.8361 \cdot 10^{-10}$	$-0.11561 + 0.18718e^{-0.53161z} + 0.13165z$	01:32:31
uDSR	$1.1703 \cdot 10^{-30}$	$0.07159\sqrt{1 + z(0.9 + (0.9 + 0.3z)z)}$	00:00:13

Table 8. Results from benchmarking the cosmological dataset C1.

B Detailed results

This section contains the raw results for the all the cosmological datasets. This means we report what the algorithm outputs, up to algebraic simplification. Numbers of the order $\mathcal{O}(10^{-10})$ or smaller are set to zero, and we round to 5 significant digits if the algorithm reports more than that. To increase readability we reduce the number of significant digits to 5 (in some cases down to 2 significant digits, see the table caption). Note that some algorithms already have a rewriting method that rounds to 5 or 6 significant digits. The runtime is given in the format HH:MM:SS (hours, minutes, seconds).

Cosmological dataset: C2			
Algorithm	MSE	Equation	Runtime
AI-Feynman	$2.0738 \cdot 10^{-4}$	$0.53006 + \log \left(\cos \left(\cos \left(\frac{1}{\pi - \sqrt{1+z}} \right) \right) \right)$	08:53:25
DSO	$2.5167 \cdot 10^{-4}$	$e^{-3+\sqrt{z}}$	01:53:07
DSR	$2.1320 \cdot 10^{-4}$	$\frac{z}{z^{1/4}+5z+2\sin(2z)}$	01:02:47
FFX	$2.0062 \cdot 10^{-4}$	$0.083 + 0.0397z + 0.0143 \max(0, -1.24 + z) + 0.00010654 \max(0, 1.75 - z) \max(0, -0.987 + z) + 0.0149 \max(0, -0.48 + z)$	00:00:08
Genetic Engine	$2.0889 \cdot 10^{-4}$	$\log \left(1 + \frac{\left \frac{-0.0041623+z(4.0623+100z)}{z-1000\log(1+ z)} \right }{\log(1+2 z)} \right)$	04:00:02
GPZGD	$5.1140 \cdot 10^{-4}$	$0.13401 + 0.043802(0.18649z(1.8686 + z)^2 + 0.153168(-4.785 + z)z \sin(\sin(z)))$	03:42:23
ITEA	$1.9684 \cdot 10^{-4}$	$0.16115 + 0.00210702z^3 - 0.0703969 \cos z - 0.00078241 \ln \left(\frac{1}{z^3} \right) + 0.0039121 \ln(z^5)$	00:07:10
PySR	$3.1870 \cdot 10^{-4}$	$0.077633z + 0.077633 \cos(\sin(z))$	00:34:39
QLattice	$1.9738 \cdot 10^{-4}$	$0.19878 - 0.16512 \tanh(1.04296 - 0.56534z)$	01:11:31
uDSR	$1.9544 \cdot 10^{-4}$	$0.931898 + z(0.278604 + z(-1.30941 + z(2.60802 + (-2.07853 + 0.576118z)z))) + \sin \left(e^{z+\cos(e^{\sin(z)})} \right)$	02:03:41

Table 9. Results from benchmarking the cosmological dataset C2.

Cosmological dataset: C3			
Algorithm	MSE	Equation	Runtime
AI-Feynman	$6.816 \cdot 10^{-6}$	$0.3902 - \frac{1}{\pi + e^z \Omega_{m,0} - \Omega_{m,0} \cos(z)}$	08:53:26
DSO	$1.871 \cdot 10^{-4}$	$e^{-e^{\frac{1}{1 + \frac{1}{\sqrt{\Omega_{m,0}}}}}} \sqrt{z \Omega_{m,0}}$	02:03:08
DSR	$1.435 \cdot 10^{-4}$	$\Omega_{m,0} \sin \left(\frac{\sqrt{e^z}}{e^{\sqrt{\Omega_{m,0} + \sqrt{2} \Omega_{m,0} + 4 \Omega_{m,0}}}} \right)$	01:18:44
FFX	$3.102 \cdot 10^{-6}$	$0.0758 + 0.00387z^2 + 0.156z\Omega_{m,0} - 0.00854\Omega_{m,0}^2 + 0.01711z \ln(z)$	00:00:33
Genetic Engine	$3.667 \cdot 10^{-5}$	$\ln \left(1 + \left -10^{-6} + \Omega_{m,0}(0.00891 + 0.99\Omega_{m,0} + z(99 \cdot 10^{-5}(1 - z) - 0.99\Omega_{m,0} + 0.99z\Omega_{m,0})) + (-0.0001 + 0.99\Omega_{m,0}) \sqrt{ z \Omega_{m,0} + 10 \ln(1 + \Omega_{m,0})} \right \right) - \ln \Omega_{m,0} + 10 \ln(1 + \Omega_{m,0}) $	04:00:02
GPZGD	$1.394 \cdot 10^{-6}$	$0.1304 + 0.004473z^2 + z(0.03948 + 0.010890\Omega_{m,0}) + \Omega_{m,0}(0.01850 - 0.001507\Omega_{m,0})$	04:00:06
ITEA	$4.226 \cdot 10^{-9}$	$0.03522 - 0.009395e^z + 0.005100z^3 + 0.08818\sqrt{z^2\Omega_{m,0}^2} + 0.07389\sqrt{ z^3\Omega_{m,0} } + 0.04640 \cos(z\Omega_{m,0})$	00:46:30
PySR	$4.354 \cdot 10^{-6}$	$0.08991(z + \cos(z\Omega_{m,0})) \sin(z\Omega_{m,0}) + 0.08991 \sin(\cos(\Omega_{m,0}))$	01:18:05
QLattice	$6.132 \cdot 10^{-9}$	$0.09638(0.5546 + e^{z(1.873+z(-0.2834+(0.01906-0.00048z)z)}) \times (10^{-4} + 0.9737\Omega_{m,0}) - \Omega_{m,0})^{1/2} - 0.00019$	01:18:05
uDSR	$2.292 \cdot 10^{-30}$	$\left((0.00512511 + z(0.0153754 + (0.0153754 + 0.00512511z)z)\Omega_{m,0}) \right)^{1/2}$	00:00:33

Table 10. Results from benchmarking the cosmological dataset C3. We include only 4 significant digits to increase readability.

Cosmological dataset: C4			
Algorithm	MSE	Equation	Runtime
AI-Feynman	$4.457 \cdot 10^{-5}$	$-0.0005896 + e^{z \sqrt{\frac{\Omega_{m,0}}{\cos(\Omega_{m,0})}}} H_0$	08:53:37
DSO	$4.142 \cdot 10^{-6}$	$H_0 + \sin\left(H_0 z \times \sqrt{\Omega_{m,0}\left(z + \left(2^{\frac{1}{4}} H_0^{\frac{1}{4}} + \sqrt{z} + z\right) \Omega_{m,0}\right)}\right)$	02:03:23
DSR	$1.267 \cdot 10^{-5}$	$e^{z \sqrt{\Omega_{m,0}}} H_0$	01:09:36
FFX	$1.396 \cdot 10^{-5}$	$0.0279 + 1.6H_0^2 - 0.0154z + 0.00453z^2 - 0.0673\Omega_{m,0} + 0.0864z\Omega_{m,0} - 0.0335\Omega_{m,0}^2 + H_0(0.253 + 0.509z + 1.76\Omega_{m,0}) + 0.0165 \max(0, -1.75 + z) + 0.0155 \max(0, -1.49 + z) + 0.0174 \max(0, -1.24 + z) + 0.0169 \max(0, -0.987 + z) + (0.382H_0 - 0.011z + 0.00573\Omega_{m,0}) \max(0, -0.733 + z) + (0.00319 + 0.118H_0 - 0.0153z + 0.0282\Omega_{m,0}) \max(0, -0.48 + z) + (0.000791 + 0.0154\Omega_{m,0} - 0.0466 \max(0, -0.48 + z)) \max(0, 0.18 - \Omega_{m,0}) + (0.000012\Omega_{m,0} - 0.0157 \max(0, -0.48 + z)) \max(0, 0.287 - \Omega_{m,0}) + \max(0, 0.0914 - H_0)(-0.0187 + 1.56H_0 - 0.105z - 0.2\Omega_{m,0} + 0.471 \max(0, 0.18 - \Omega_{m,0}) + 0.295 \max(0, 0.287 - \Omega_{m,0}) + 0.124 \max(0, 0.34 - \Omega_{m,0}) + (-0.0241z + 0.0494\Omega_{m,0}) \max(0, 0.34 - \Omega_{m,0})$	00:04:25
Genetic Engine	$8.032 \cdot 10^{-6}$	$\ln\left(1 + \left 2H_0^2(1+z) + 0.01z\Omega_{m,0} + H_0(0.02 + z(1+z)\Omega_{m,0}) + \log\left(1 + \left \frac{H_0}{1+H_0}\right \right)\right \right)$	04:00:03
GPZGD	$4.286 \cdot 10^{-5}$	$0.1143 + 0.02788(-0.2847 + 2.635z + H_0(3.624 + z - 0.5\Omega_{m,0}) + 1.191\Omega_{m,0})(0.4654 + \sin(0.001689H_0 + 0.1178\Omega_{m,0}))$	04:02:59
ITEA	$5.052 \cdot 10^{-8}$	$-0.00006954 + 1.596\sqrt{H_0^2 z^2 \Omega_{m,0}^2} + \sqrt{H_0^2}((-0.03965 - 0.3329\Omega_{m,0}^2) z ^{5/2} + 0.6482z^2\sqrt{ \Omega_{m,0} }) + 0.9949 \sin(H_0)$	09:50:16
PySR	$3.268 \cdot 10^{-6}$	$H_0 + H_0(H_0 + z^2 + \sin(z))(0.09293 + \sin(\Omega_{m,0}))$	06:01:51
QLattice	$6.005 \cdot 10^{-7}$	$e^{-1.224e^{-\frac{1.279}{-0.4023+z(1.269+z)}} - (2.494+3.169\Omega_{m,0})\Omega_{m,0}}$	04:09:02
uDSR	$3.355 \cdot 10^{-29}$	$e^{(0.9798-0.1242z)z(0.00004588 + 0.9823H_0)} \times 1.732H_0\sqrt{0.3333 + z(1+z + 0.3333z^2)\Omega_{m,0}}$	00:01:17

Table 11. Results from benchmarking the cosmological dataset C4. To increase readability, we only include 4 significant digits.

Cosmological dataset: C5			
Algorithm	MSE	Equation	Runtime
AI-Feynman	$1.3715 \cdot 10^{-10}$	$0.071568 - H + 0.071611z$	08:53:26
DSO	$3.6475 \cdot 10^{-4}$	$e^{-e^{\cos H} - H + \sqrt{z}} - H$	03:02:26
DSR	$1.5928 \cdot 10^{-4}$	$-2H + \sin\left(\frac{(H^2z)^{1/4}}{e^{1/4}}\right)$	01:20:14
FFX	$8.4654 \cdot 10^{-6}$	$0.0704 - 0.946H + 0.066z$	00:00:20
Genetic Engine	$3.9676 \cdot 10^{-5}$	$1/\left(H(-0.01 + z)z \log(1 + z)\right) \times$ $\left(H(H^2(0.002 - 0.2z) + 0.01z^2 -$ $0.1Hz^2 + H^3(-0.02 + 2z)) +$ $(0.028748Hz^2 + H^3(0.0057496 +$ $(-0.55965 - 1.5311z)z) + (-0.00031623 +$ $0.031623z)z^2 \log(1 + 0.1 z) \log(1 + z)\right)$	04:00:03
GPZGD	$1.6298 \cdot 10^{-31}$	$0.017062 - 0.05722H + 0.0395799z$	04:00:04
ITEA	$1.5181 \cdot 10^{-32}$	$0.07159 - H + 0.07159z$	00:37:57
PySR	$1.0775 \cdot 10^{-31}$	$0.07159 - H + 0.07159z$	01:19:06
QLattice	$2.1592 \cdot 10^{-18}$	$0.07159 - H + 0.07159z$	01:34:42
uDSR	$2.1666 \cdot 10^{-30}$	$0.07159 - H + 0.07159z$	00:00:33

Table 12. Results from benchmarking the cosmological dataset C5.

Cosmological dataset: C6			
Algorithm	MSE	Equation	Runtime
AI-Feynman	$2.5761 \cdot 10^{-3}$	$0.00061452\sqrt{\cos(z - \omega)}$	08:53:26
DSO	$8.7609 \cdot 10^{-4}$	$e^{-2z}z^3\omega \sin(\omega)$	02:14:18
DSR	$8.2501 \cdot 10^{-4}$	$z\omega \cos(\omega)(\omega - \sin(\omega))$	01:02:51
FFX	$8.3131 \cdot 10^{-6}$	$0.00088 + z(-0.0127 - 0.00114z - 0.0861\omega) + (-0.0058z - 0.152\omega) \max(0, 0.264 + \omega) + (0.0113 - 0.14z - 0.0676\Omega) \max(0, 0.396 + \omega) + 0.0596\omega \max(0, 0.66 + \omega) + 0.00984\omega \max(0, 0.792 + \omega)$	00:00:29
Genetic Engine	$3.2259 \cdot 10^{-5}$	$\frac{1}{(0.1+z)\sqrt{ \omega }\sqrt{ \ln(2) - \frac{0.01}{\omega} }} \times (0.00001 + z(-0.000911 + (-0.009019 - 0.00009z)z) + (10^{-7} - 0.0001z^4 + z^3(-0.010021 - 0.00101\omega) + (0.000011 + 0.0001\omega)\omega + z(9.9 \cdot 10^{-7} + (-0.0000911 - 0.01001\omega)\omega) + z^2(-0.0010012 + (-0.10111 - 0.0001\omega)\omega))\sqrt{ \omega })$	04:00:03
GPZGD	$5.8316 \cdot 10^{-7}$	$0.017062 + 0.048862(1.82618 - \omega + 0.30712(2.7244 + z)(-0.617711 + \omega)(6.07434 + \omega) + \sin(2.20643 - \omega) - \sin(\omega))(-0.25093 - 0.017332z - 0.0222548 \sin(z) \sin(\omega))$	04:00:11
ITEA	$1.7575 \cdot 10^{-7}$	$0.010554 - 0.015561e^\omega + (-0.0543818 + \sqrt{\omega^2}(0.20119 + 0.0232074 z)) z ^{3/2} - 0.10277z^2 \omega ^{3/2}$	00:30:54
PySR	$1.0410 \cdot 10^{-5}$	$z(-0.064556 - 0.199302 \sin(\sin(\sin(\omega))))$	01:18:13
QLattice	$1.3879 \cdot 10^{-16}$	$0.07159 + 0.07159z - 0.07159(1 + z)^{1.5+1.5\omega}$	01:19:57
uDSR	$4.4729 \cdot 10^{-8}$	$z(-0.029821 + z^2(-0.0059464 - 0.015213\omega) + \omega(-0.076830 + 0.025993\omega - 0.011582\omega^3) + z(-0.012088 + \omega(-0.079478 + (-0.12207 - 0.041603\omega)\omega)))\sqrt{\sqrt{z} + \cos(z)}$	08:04:58

Table 13. Results from benchmarking the cosmological dataset C6.

Cosmological dataset: C7			
Algorithm	MSE	Equation	Runtime
AI-Feynman	$2.7984 \cdot 10^{-6}$	$-0.34629 + 2z + \sin(\ln(1 + 1/\sqrt{z}))$	08:53:25
DSO	$1.1025 \cdot 10^{-4}$	$e^{\sin(\sqrt{z^{9/4}})} \sin(z)^{1/8}$	01:51:17
DSR	$9.4667 \cdot 10^{-5}$	$\sqrt{z + \left(\sqrt{\sqrt{z}\sqrt{z^2}\sqrt{\sqrt{z} + z}}\right)^{1/4}} + \sin(z^2)$	01:22:39
FFX	$1.8697 \cdot 10^{-4}$	$0.854 + 1.07z - 0.106 \max(0, 0.88 - z) +$ $0.00322 \max(0, -0.64 + z) +$ $0.0764 \max(0, -0.52 + z) +$ $0.0869 \max(0, -0.4 + z) +$ $0.329 \max(0, -0.28 + z)$	00:00:09
Genetic Engine	$7.7503 \cdot 10^{-6}$	$-0.0101 + \frac{0.01}{(-0.001+z)} + z + \sqrt{\ln(1 + z ^{1/4})} +$ $\ln(1 + -0.1 + z) (0.01z + \ln(1 + z))$	04:00:02
GPZGD	$2.3718 \cdot 10^{-10}$	$1.5248 - 0.071297(-1.858 + z +$ $3.1905 \sin(0.19116 - 0.31729z))(-1.7455 +$ $z(3.7687 + z) + 1.85786 \sin(0.95534 + z))$	04:00:01
ITEA	$4.2795 \cdot 10^{-13}$	$0.90149 + 0.53752z^2 + 0.018102z^4 -$ $0.51308\sqrt{ z } + 0.021246 \ln(z) + 1.5975 \sin(z)$	00:07:34
PySR	$3.3619 \cdot 10^{-7}$	$-0.25753 + 1.4661z^2 + (1 + z) \cos z$	00:39:03
QLattice	$6.3230 \cdot 10^{-11}$	$0.84231 + (0.1493 - 1.6947z) \tanh(0.28708 -$ $0.98918z - \tanh(1.3646 + 4.01013z))$	01:24:10
uDSR	$4.1879 \cdot 10^{-13}$	$\left((0.50883 + z(2.16401 +$ $z(11.0341 + z(9.92183 + (31.6592 -$ $4.58133z)z))) \cos(\sin(z + \cos(z))) \right)^{1/4}$	02:02:22

Table 14. Results from benchmarking the cosmological dataset C7.

Cosmological dataset: C8			
Algorithm	MSE	Equation	Runtime
AI-Feynman	$1.4727 \cdot 10^{-4}$	$1.74408 \left(-1 + \cos \left(\ln \left(\frac{z}{1 + \cos(\cos(\sqrt{z}))} \right) \right) \right)$	08:53:25
DSO	$6.0531 \cdot 10^{-3}$	$-e^{\cos(\sqrt{z})} + \sqrt{z} + \cos\left(\frac{1}{\sqrt{z}}\right)$	02:01:01
DSR	$6.3937 \cdot 10^{-4}$	$\frac{z - \sqrt{\cos(z)} - 2 \cos(z)}{3z + \cos(\sqrt{1+z})}$	00:54:03
FFX	$2.0215 \cdot 10^{-4}$	$\frac{-1.3112 + 0.70091z}{0.30212 + z(0.53112 + z)}$	00:00:07
Genetic Engine	$4.6980 \cdot 10^{-4}$	$\frac{1}{(0.01+z)(-0.0075724+z(-0.024276+z))} \times$ $\frac{1}{(0.13206+z(-1.7439+z(9.8243+1.z)))^2} \times \left(0.00001258 + \right.$ $z(-0.00029719 + z(-0.000095321 + z(0.081972 +$ $z(-1.2064 + z(7.55163 + z(-16.908 + z(-28.497 +$ $z(100.011 + z(0.899891 + (-2.93686 -$ $0.2z)z)))))) - \frac{0.99\sqrt{ z }}{0.01+z}$	04:00:02
GPZGD	$5.0238 \cdot 10^{-7}$	$1.5643 + z^2(0.028230 + (0.17824 - 0.040466z)z) +$ $0.863365 \sin(0.652812 + z)$	03:19:41
ITEA	$1.0773 \cdot 10^{-10}$	$-117.78 - 37.117z^3 + 79.351 z ^{5/2} + 112.87 \cos(z) +$ $0.082433 \cos(z^4) + 16.8726 \sin(z)$	00:07:32
PySR	$6.5462 \cdot 10^{-6}$	$\frac{-1.6633+z}{-0.65998+e^z}$	00:37:20
QLattice	$6.3230 \cdot 10^{-9}$	$0.18811 - \frac{4.76604}{-0.0482153+e^{(2.59213-0.41332z)z}+0.49838z}$	01:22:29
uDSR	$3.6453 \cdot 10^{-11}$	$\frac{7.2424e^{-z} \cos(z - \cos(z))}{-0.81024+z(-3.2244+z(-3.6363+z(-2.1385+z(1.4662+z))))}$	02:06:11

Table 15. Results from benchmarking the cosmological dataset C8.

Cosmological dataset: C9			
Algorithm	MSE	Equation	Runtime
AI-Feynman	$1.7755 \cdot 10^{-3}$	$5.723 \sin(\sin(f_o(1 + f_o - \cos(e^z))))$	08:53:25
DSO	$3.2599 \cdot 10^{-3}$	$4f_o(1 + z + z^2)$	01:46:58
DSR	$2.3962 \cdot 10^{-3}$	$f_o(4 + (4 + e^z)z + z \sin(z))$	01:30:05
FFX	$4.7415 \cdot 10^{-4}$	$0.247 + 1.48f_o^2 + (0.0229 + 0.33z)z + f_o(3.09 +$	00:00:14
Genetic Engine	$4.2219 \cdot 10^{-4}$	$5.93z) + 0.11769 \ln(f_o)$ $\frac{9.95037}{\sqrt{ (0.1+z)}} \sqrt{\log(1 + z)} \times$	04:00:03
GPZGD	$9.3926 \cdot 10^{-5}$	$\sqrt{ (f_o(-0.01 + f_o + z^2)(-0.101 + \sqrt{ f_o })) }$ $1.30095 - 0.013081f_o^2z + (0.39948 +$	04:00:02
ITEA	$1.1606 \cdot 10^{-6}$	$0.026055z)z + f_o(0.34708 + (0.063779 -$ $0.0047181z)z)$ $0.077995 + 43.919f_o^4z^5 + 7.5085 f_2 ^{3/2} -$	00:15:28
PySR	$178394 \cdot 10^{-3}$	$372.78 f_o z + 377.62 \sin(f_oz) +$ $5.059 \sin(f_oz^2)$	00:43:52
QLattice	$2.6170 \cdot 10^{-6}$	$-(-3.1935 + f_o)f_o(e^z + f_o + z)$ $\exp(f_o(26.254 + f_o(-95.967 + (214.09 -$	01:21:19
uDSR	$1.4228 \cdot 10^{-7}$	$193.26f_o)f_o)) + 2.1979z + f_o(-2.5315 +$ $(-1.7758 - 0.25197f_o)f_o)z + (-0.38712 +$ $(-0.20255 - 0.0265f_o)f_o)z^2)$ $f_o(-f_o - \sqrt{z} + (18.188z)/(f_o^4(-0.00080365 -$	08:56:52
		$0.0024583z) - 0.00029248f_o^2z^2 +$ $f_o^3(-0.00031865 + z(-0.0040394 + 8.4073z)) +$ $f_oz(-7.4686 + z(16.914 + z(-12.9 + 3.869z))) +$ $z(5.9143 + z(-10.329 + z(9.4388 + z(-4.7351 +$ $z))))))$	

Table 16. Results from benchmarking the cosmological dataset C9.

Cosmological dataset: C10			
Algorithm	MSE	Equation	Runtime
AI-Feynman	$5.5780 \cdot 10^{-3}$	$-3.31857 \left(1 + \ln \left(\frac{\cos(1+f_o)}{\sqrt{\sin(z)}} \right) \right)$	08:53:25
DSO	$4.7046 \cdot 10^{-2}$	$-e^{\cos(e^{f_o+z})+\cos(z)} + f_o$	02:09:10
DSR	$5.1333 \cdot 10^{-2}$	$z + \cos \left(e^{f_o+f_o(e^z+2f_o)z^{3/2}} \right)$	01:26:32
FFX	$1.1563 \cdot 10^{-3}$	$\frac{-1.109+0.24877z+f_o(1.6621+3.2234f_o+1.0082z)}{0.27248+(0.21063+0.10872z)z+f_o(-0.73297+z)}$	00:00:14
Genetic Engine	$4.8526 \cdot 10^{-3}$	$\frac{-0.969377+(0.002+2 \cdot f_o)z+\sqrt{ 0.1+f_o }\sqrt{\ln(1+ z)}}{\ln(1+\sqrt{ 0.01+0.1z+f_o(0.1+z) })}$	04:00:02
GPZGD	$1.1148 \cdot 10^{-3}$	$-1.20718 + f_o(0.36614 + (-0.01031 - 0.039932z)z) + z(0.70714 + (-0.29968 + 0.083566z)z)$	04:00:03
ITEA	$2.4749 \cdot 10^{-5}$	$-1.404 + 14.347 f_o ^{5/2} + \frac{0.1158}{ z } + 16.604 f_o \sqrt{ z } - 1.8608 \ln \left(\frac{1}{z} \right) - 13.189 \sin(f_o z)$	00:13:36
PySR	$1.5662 \cdot 10^{-2}$	$(-1 + 6.3985f_o)z - \frac{\cos(z^2)}{f_o+z}$	00:49:22
QLattice	$1.4790 \cdot 10^{-5}$	$0.92085 + \frac{7.7295}{-1.1407+f_o-1.9551z} + 0.58269e^{(9.067-8.8869f_o)f_o+(-0.45659-0.11034z)z}$	01:25:34
uDSR	$1.2834 \cdot 10^{-6}$	$\frac{1}{f_o-\sqrt{\cos(\cos(z^2))}} \left(3.9998 + f_o^4(-0.033227 - 0.0048309z) + f_o^3(-0.011253 + (-0.0077552 - 0.00045493z)z) + f_o^2(-0.000025891 + z(-0.0011397 + (-0.00058458 - 0.000041934z)z)) + f_o(-7.2986 + z^2(13.032 + z(-18.308 + 7.3428z))) + z(-7.8979 + z(10.875 + z(-10.587 + (7.1956 - 2.304z)z))) \right)$	08:10:39

Table 17. Result from benchmarking the cosmological dataset C10.

Cosmological dataset: C11			
Algorithm	MSE	Equation	Runtime
AI-Feynman	$2.1808 \cdot 10^{-3}$	$2.04061e^{\sec(1+\Omega_{Q,0}) \sin(z)} \Omega_{m,0}$	08:53:25
DSO	$1.2224 \cdot 10^{-3}$	$2\Omega_{m,0} + z (\Omega_{m,0} + \sqrt{2\Omega_{m,0} + 2z\Omega_{m,0}})$	01:50:32
DSR	$1.2318 \cdot 10^{-3}$	$2\Omega_{m,0} + z \left(\sqrt{2} \sqrt{\Omega_{m,0}} + \sqrt{\Omega_{m,0} (\Omega_{m,0} + z \sqrt{\sin(2\Omega_{m,0})})} \right)$	01:41:27
FFX	$5.6198 \cdot 10^{-4}$	$0.976 + z(0.0709 + 0.341z - 3.94\Omega_{Q,0}) - 0.861\Omega_{Q,0} + \ln(z)(0.12464z - 0.041117 \ln(\Omega_{m,0})) + \ln(\Omega_{m,0})(0.35569 + 0.43758 \ln(\Omega_{R,0}))$	00:00:22
Genetic Engine	$1.3613 \cdot 10^{-3}$	$\left((0.00031623 + 0.031623z)z^5 + 0.001\Omega_{m,0} + z^2 \ln(1 + \ln(1 + \Omega_{Q,0})) \right) / \left(z^2 \ln(1 + \frac{0.1}{\sqrt{ z(-0.01 + \Omega_{R,0}) }}) \right)$	04:00:02
GPZGD	$5.8433 \cdot 10^{-4}$	$1.3252 + 0.51604 \times (\sin(\Omega_{Q,0}(0.21285 - 0.11323\Omega_{R,0})) + 0.062808 \times (z + 1.1475\Omega_{m,0})(12.13 + z - \sin(\Omega_{R,0})))$	04:00:02
ITEA	$4.5589 \cdot 10^{-7}$	$-243.902 + 0.0275e^{\frac{H_0\Omega_{Q,0}^3}{z^2\Omega_{m,0}^5\Omega_{R,0}}} + 250.25e^{\frac{H_0z^2\Omega_{Q,0}^4\Omega_{R,0}^5}{\Omega_{m,0}^3}} - \frac{0.6278 \Omega_{Q,0} \Omega_{R,0} }{ H_0^{5/2}\Omega_{m,0} } + 369.6\sqrt{\left \frac{H_0^3z^2\Omega_{Q,0}^4\Omega_{R,0}^3}{\Omega_{m,0}^2} \right } - 1.1548 \sin\left(\frac{z^3\Omega_{m,0}^4\Omega_{R,0}}{\Omega_{Q,0}^2}\right)$	00:21:57
PySR	$1.2605 \cdot 10^{-3}$	$2\Omega_{m,0} + (z + 2\Omega_{m,0} - \Omega_{Q,0}) \sin(\sin(z))$	01:01:31
QLattice	$2.2399 \cdot 10^{-6}$	$0.03285 + 4.6164 \tanh\left(0.28715 \exp\left(0.33924z^2 + (-4.6641 - 1.8771\Omega_{Q,0})\Omega_{Q,0} + z(1.9828 + 1.596\Omega_{Q,0}) - 0.39264 \ln(0.33295 + 8.651\Omega_{m,0})^2\right)(0.03849 + \Omega_{m,0})^{1.1649}\right)$	01:24:51
uDSR	$4.1677 \cdot 10^{-3}$	$e^{2\Omega_{m,0} + \Omega_{Q,0}}(z + \Omega_{m,0})$	05:51:49

Table 18. Result from benchmarking the cosmological dataset C11.

Cosmological dataset: C12			
Algorithm	MSE	Equation	Runtime
AI-Feynman	$1.7502 \cdot 10^{-4}$	$-6.60223 \left(\Omega_{R,0} - \sin \left(\sqrt{\sin \left(\frac{z}{1+\Omega_{Q,0}} \right)} \right) \right)$	08:53:26
DSO	$2.5639 \cdot 10^{-2}$	$\frac{(z+\Omega_{m,0}-2\Omega_{R,0})\Omega_{R,0}}{\sqrt{z}}$	02:16:06
DSR	$8.3090 \cdot 10^{-3}$	$-e^{\cos(4z)} + z - \Omega_{Q,0} - \cos(\sqrt{\Omega_{m,0} + 2\Omega_{m,0}}) - \cos(\Omega_{Q,0})$	01:11:15
FFX	$1.5102 \cdot 10^{-3}$	$0.985 + 0.19\Omega_{m,0} - 1.03\Omega_{Q,0} - 2.42\Omega_{R,0} + 1.46 \Omega_{Q,0} + 1.0684 \ln(z) - 1.1205 \ln(\Omega_{R,0}) - 0.413 \max(0, 0.4 - z) - 0.472 \max(0, 0.52 - z) - 0.329 \max(0, 0.64 - z) - 0.248 \max(0, 0.76 - z)$	00:00:20
Genetic Engine	$3.2492 \cdot 10^{-2}$	$\frac{1}{z\Omega_{Q,0}\sqrt{\left \frac{(H_0+z)\Omega_{Q,0}}{-1+z}\right }} (\Omega_{Q,0}(0.00010207 + \Omega_{Q,0}(0.0010207 + 0.10207\Omega_{R,0}) + 0.010207\Omega_{R,0}) + H_0(-0.00010207 - 0.010207\Omega_{R,0} + \Omega_{Q,0}(0.00010207 - 0.10207z + 0.010207\Omega_{R,0} - 10.207z\Omega_{R,0})))$	04:00:03
GPZGD	$1.1023 \cdot 10^{-1}$	$-2.0208 + 0.941606z + 0.941606 \sin(1.7203 + z)$	04:00:02
ITEA	$3.7904 \cdot 10^{-6}$	$64.407 - 4.7363e^{\frac{H_0\Omega_{Q,0}\Omega_{R,0}^3}{z\Omega_{m,0}}} - 0.0048491\sqrt{\left \frac{z^5\Omega_{Q,0}^3}{H_0^5\Omega_{m,0}^2}\right } - 115231\sqrt{\left \frac{H_0^5\Omega_{Q,0}^5}{\Omega_{m,0}^5}\right } - 1.1064 \ln\left(\frac{\Omega_{Q,0}^4\Omega_{R,0}^5}{z^2\Omega_{m,0}^4}\right) + 1.2291 \sin\left(\frac{z^4\Omega_{m,0}^3\Omega_{R,0}^5}{\Omega_{Q,0}^2}\right)$	00:20:01
PySR	$2.6913 \cdot 10^{-3}$	$3\Omega_{m,0} - \frac{\cos(z)}{0.16193+z} - \cos(\Omega_{m,0})$	01:02:47
QLattice	$5.5227 \cdot 10^{-6}$	$-6.7966 + (4.9988 - 1.3031z)z + (17.126 - 14.309\Omega_{R,0} + z(-6.4144 + 5.3595\Omega_{R,0})) \tanh(0.51617 + 2.7524z)$	01:23:43
uDSR	$6.4092 \cdot 10^{-2}$	$-\frac{1}{\sqrt{z}} + z + \Omega_{m,0} - \Omega_{R,0}$	06:42:47

Table 19. Result from benchmarking the cosmological dataset C12.

Cosmological dataset: C13			
Algorithm	MSE	Equation	Runtime
AI-Feynman	$1.0899 \cdot 10^{-3}$	$\frac{9.52774v}{v+\sin(e^h+H)}$	08:53:26
DSO	$1.3183 \cdot 10^{-2}$	$\frac{v}{\sqrt{e^{h+H}} \sin(H)}$	02:18:15
DSR	$8.5126 \cdot 10^{-3}$	$3v + \sqrt{\sin(\sqrt{v})} + \sin(e^{-e^v(-1+h+v)}v)$	01:28:53
FFX	$4.1661 \cdot 10^{-4}$	$1.47 + (2.52 + 0.955v)v - 0.110311 \ln(H) +$ $0.212804 \ln(v) + 154v \max(0, 0.0952 - H) +$ $\max(0, 0.0875 - H) (266.v$ $1447. \max(0, 0.0952 - H))$ $64.9v \max(0, 0.103 - H)$ $28.4v \max(0, 0.111 - H) + (16.5v$ $28.2 \max(0, 0.111 - H)) \max(0, 0.119 - H) -$ $0.877 \max(0, 0.242 - v)$ $0.492 \max(0, 0.294 - v)$ $1.04 \max(0, 0.346 - v)$	00:00:20
Genetic Engine	$4.9531 \cdot 10^{-4}$	$\ln(1 + 0.001 + H + 2v + 10h^2v)$	04:00:02
GPZGD	$1.5478 \cdot 10^{-3}$	$\frac{\ln(1+\ln(1+ -0.01+v))}{\ln(1+ -0.001+H+0.1v)}$ $1.3717 - 0.36614H + 0.90411v + (-0.051963 +$ $0.40895H - 0.51604v) \sin(h)$	04:00:02
ITEA	$1.0126 \cdot 10^{-5}$	$-730.086 + 730.07e^{H^2v} + \frac{0.00001566v}{H^5} -$ $1213.8hH^2v + 3.4928 h ^2 v - 91.103\sqrt{ H^5v }$	00:12:50
PySR	$4.7100 \cdot 10^{-4}$	$-\frac{v(h-13.85H+hH+\cos(\cos(v)))}{H}$	00:47:21
QLattice	$4.7471 \cdot 10^{-6}$	$-0.01493 + (9.2758 - 4.3376v)v + (0.00366 -$ $4.5621v) \ln(e^{(1.7333-0.7552h)h+(4.5425-49.63H)H})$	01:24:48
uDSR	$1.4753 \cdot 10^{-2}$	$\frac{v}{\sqrt{e^hH}}$	06:22:24

Table 20. Result from benchmarking the cosmological dataset C13.

Cosmological dataset: C14			
Algorithm	MSE	Equation	Runtime
AI-Feynman	$4.8209 \cdot 10^{-4}$	$\frac{3.503\Omega_{m,0}}{\ln\left(\Omega_{m,0} - \frac{1}{\ln(\sin(a_D))}\right)}$	08:53:26
DSO	$2.0520 \cdot 10^{-3}$	$\Omega_{m,0} + \frac{\Omega_{m,0}}{a_D \sin(a_D) \sin(a_D + \Omega_{m,0})}$	01:37:21
DSR	$1.6317 \cdot 10^{-3}$	$\Omega_{m,0} + \frac{\Omega_{m,0}}{a_D^2 (\Omega_{m,0} (a_D + \Omega_{m,0}))^{1/4}}$	00:52:37
FFX	$4.7861 \cdot 10^{-4}$	$-0.515 - 68100\ddot{a}_D^2 + 49.8H^2 + 119\ddot{a}_D\Omega_{m,0} + 45.4H\Omega_{m,0} - 0.768\Omega_{m,0}^2$	00:00:18
Genetic Engine	$3.4552 \cdot 10^{-4}$	$\frac{10\ddot{a}_D}{a_D^2} + \frac{0.001a_D}{\Omega_{m,0}^2} + (0.001 + a_D^2 H(0.01 - 0.1\Omega_{m,0}) + (-0.02 + 0.1\Omega_{m,0})\Omega_{m,0} + H(0.0099 + \Omega_{m,0}(-0.199 + \Omega_{m,0})) + a_D(-0.0001 - 0.001H^2 + \ddot{a}_D(0.01 + \Omega_{m,0}(-0.2 + \Omega_{m,0})) + \Omega_{m,0}(0.022 + \Omega_{m,0}(-0.41 + 2\Omega_{m,0})))) / ((0.001 + 0.01a_D H + a_D^2(-0.1 + \Omega_{m,0}) - 0.01\Omega_{m,0})(-0.1 + \Omega_{m,0})) - \frac{0.011}{\ln(1+ H)}$	04:00:02
GPZGD	$1.8595 \cdot 10^{-5}$	$1.3252 + 0.089988(-45.993 - 1.9563\ddot{a}_D + a_D(-5.7345 + \ddot{a}_D) - 18.469H)(0.019835 + \sin(0.10711a_D - 0.089082\Omega_{m,0}))$	04:00:03
ITEA	$1.4753 \cdot 10^{-2}$	$-1.1598 \cdot 10^{-9} + \frac{300\ddot{a}_D}{a_D} + \frac{0.76877\Omega_{m,0}}{a_D^3} - 1.3366 \cdot 10^{-9} \cos\left(\frac{1}{H\Omega_{m,0}}\right) - 1.5418 \cdot 10^{-9} \cos\left(\frac{\Omega_{m,0}^4}{a_D H^3}\right) + 1.3769 \cdot 10^{-9} \sin\left(\frac{\Omega_{m,0}^4}{H^4}\right)$	00:17:56
PySR	$1.4508 \cdot 10^{-3}$	$\Omega_{m,0} + \frac{H + \Omega_{m,0}}{a_D^2 + \Omega_{m,0}^6}$	00:50:47
QLattice	$1.3038 \cdot 10^{-6}$	$\exp\left((-0.00054e^{(2.8015-3.6795a_D)a_D} \times (e^{26.6842H})e^{-30.4281H^2} + (-0.46521 - 0.24078\Omega_{m,0})\Omega_{m,0} + e^{(2.8015-3.6795a_D)a_D + (26.684-30.428H)H} \times (-0.05175 - 0.053\Omega_{m,0})\Omega_{m,0} + e^{(5.603-7.3591a_D)a_D + (53.368-60.856H)H} \times (-3.1924 \cdot 10^{-7} + (-0.000061024 - 0.00292\Omega_{m,0})\Omega_{m,0})\right)$	01:27:28
uDSR	$2.7045 \cdot 10^{-3}$	$\frac{2.71828\Omega_{m,0}}{a_D(a_D + \Omega_{m,0})}$	06:41:02

Table 21. Result from benchmarking the cosmological dataset C14.

Cosmological dataset: C15			
Algorithm	MSE	Equation	Runtime
AI-Feynman	16.477	$14.14 - 2.718e^{\sqrt{e^{1+\langle z \rangle}}} - \langle z \rangle$	08:53:25
DSO	16.184	$-e^{e^{\langle z \rangle}} + e^{e^{\langle z \rangle} \cos(\sqrt{\langle z \rangle})} - 11 \langle z \rangle$	02:12:41
DSR	16.106	$e^{e^{\langle z \rangle}} - e^{4\langle z \rangle + \cos(2\langle z \rangle)} - 4 \langle z \rangle$	01:33:26
FFX	16.128	$-0.414 - 12.9 \langle z \rangle$	00:00:22
		$3.48 \max(0, -0.733 + \langle z \rangle)$	–
		$3.38 \max(0, -0.6 + \langle z \rangle)$	–
		$2.84 \max(0, -0.467 + \langle z \rangle)$	–
		$3.89 \max(0, -0.333 + \langle z \rangle)$	–
		$5.69 \max(0, -0.2 + \langle z \rangle)$	–
Genetic Engine	16.054	$\left(\langle z \rangle \left(-0.0000999 + 0.101 \langle z \rangle - \langle z \rangle^2 \right) \langle z \rangle ^{\frac{3}{2}} + \langle z \rangle (0.0009511 + \langle z \rangle (-0.9616 + \langle z \rangle (9.52 + \langle z \rangle (-0.0889 + 99 \langle z \rangle))) + \langle z \rangle (-0.0000999 + 0.101 \langle z \rangle - \langle z \rangle^2) \ln(1 + \langle z \rangle)) + \langle z \rangle (-0.01 + \langle z \rangle) (-0.0009511 + (1.903 - 952.06 \langle z \rangle) \langle z \rangle + \langle z \rangle (0.0000999 + \langle z \rangle (-0.1999 + 100 \langle z \rangle)) \ln(1 + \langle z \rangle)) + \sqrt{ \langle z \rangle } (-9.511 \cdot 10^{-6} + \langle z \rangle (0.009616 + \langle z \rangle (0.8464 + \langle z \rangle (-942.5 + \langle z \rangle (-1.2 + 100 \langle z \rangle)))) + \langle z \rangle (9.99 \cdot 10^{-7} + \langle z \rangle (-0.00101 + \langle z \rangle (-0.0889 + 99 \langle z \rangle))) \ln(1 + \langle z \rangle)) / (\langle z \rangle^2 \sqrt{ \langle z \rangle } (9.521 - \langle z \rangle \sqrt{ \langle z \rangle } - \langle z \rangle \ln(1 + \langle z \rangle))^2) \right)$	04:00:03
GPZGD	17.002	$-12.298 + \langle z \rangle (-1.5047 + \langle z \rangle (-7.639 \cdot 10^{-6} + \langle z \rangle (1.605 + (0.3499 - 0.9635 \langle z \rangle) \langle z \rangle))) - 8.23 \sin(16.181 - \langle z \rangle)$	04:00:09
ITEA	16.049	$0.4798 - 5.6346 \sqrt{ \langle z \rangle } - 22.81 \sin(\langle z \rangle^2)$	00:17:48
PySR	18.322	$-21.601z \langle z \rangle$	01:23:46
QLattice	16.045	$0.1701 + (-10.99 - 13.93 \langle z \rangle) \langle z \rangle$	01:18:43
uDSR	16.115	$-14.973 \langle z \rangle + 17.457 \langle z \rangle^2 - 87.6 \langle z \rangle^3 + 100.9 \langle z \rangle^4 - 40.81 \langle z \rangle^5 + \cos\left(\cos e^{e^{\langle z \rangle}} \langle z \rangle\right)$	04:45:25

Table 22. Result from benchmarking the cosmological dataset C15. To increase readability, we only include 4 significant digits.

Cosmological dataset: C16			
Algorithm	MSE	Equation	Runtime
AI-Feynman	3.0829	$18.16 + \frac{\pi}{\ln(\sin(1+(-1+e^{f_o})\langle z \rangle))}$	08:53:25
DSO	$8.0794 \cdot 10^{-1}$	$-e^{2\langle z \rangle + 7f_o} + e^{-\langle z \rangle + \cos(\sqrt{\langle z \rangle})}$	02:02:58
DSR	$6.5251 \cdot 10^{-1}$	$-e^{e^{2f_o} + \langle z \rangle^{1/4} + 4f_o} \langle z \rangle + f_o$	01:24:34
FFX	$1.6590 \cdot 10^{-1}$	$-0.189 - 1.21 \max(0, -0.6 + \langle z \rangle) - 70.3 \langle z \rangle f_o - 1.9 \max(0, -0.467 + \langle z \rangle) + \max(0, -0.2 + \langle z \rangle) (-36.6 f_o - 7.3 \max(0, -0.21 + f_o) - 96 \max(0, -0.15 + f_o) + \max(0, -0.733 + \langle z \rangle) (-38.6 f_o - 56.2 \max(0, -0.15 + f_o)) - 0.992 \langle z \rangle \max(0, -0.15 + f_o)$	00:00:24
Genetic Engine	$5.8377 \cdot 10^{-2}$	$(f_o(f_o((-0.001 - 0.01 f_o) f_o + \langle z \rangle^5 (-0.02 + 2 f_o) + \langle z \rangle (-0.001 + f_o(1.09 + f_o)) + \langle z \rangle^4 (3 + f_o(-100 + 1.98 f_o)) + \langle z \rangle^3 (-100 + f_o(3.07 + (-99.1 - 0.02 f_o) f_o)) + \langle z \rangle^2 (1.1 + f_o(-99.1 + f_o 0.07 + f_o)))) + (-0.00001 - 0.0001 f_o + \langle z \rangle (0.01 + 2 \cdot 10^{-6} f_o + \langle z \rangle (0.0998 + (1 + 0.01 f_o) f_o + \langle z \rangle^3 (-0.02 + 2 f_o) + \langle z \rangle^2 (3 + (-100 - 0.02 f_o) f_o) + \langle z \rangle (-100 + f_o(-0.93 + f_o)))))) \sqrt{ \langle z \rangle }) \times \frac{1}{\langle z \rangle (\langle z \rangle + 0.01 f_o)}$	04:00:02
GPZGD	$4.1027 \cdot 10^{-2}$	$-8.133 - 2.797 f_o + \langle z \rangle (-6.96 - 1.124 \langle z \rangle - 2.357 f_o - 0.4067 \langle z \rangle f_o) + (-8.23 \langle z \rangle - 0.464 f_o) \sin(3.23 - f_o) + \sin(\langle z \rangle) (-0.402 + 8.23 \sin(f_o))$	04:00:27
ITEA	$3.5556 \cdot 10^{-2}$	$294 - 294.4 e^{\langle z \rangle f_o^3} - 52.82 \sin(\langle z \rangle f_o) + \frac{0.09647 - 308.5 \langle z \rangle ^2 f_o ^3}{\sqrt{ f_o }} - 51.31 \sin(\langle z \rangle^2 f_o)$	00:48:46
PySR	$6.8305 \cdot 10^{-2}$	$\langle z \rangle f_o (-70.73 - 363.6 \langle z \rangle f_o)$	01:25:13
QLattice	$3.5835 \cdot 10^{-2}$	$(0.08902 - 0.1412 f_o + \langle z \rangle (-0.1025 + 31.27 f_o + \langle z \rangle (-0.1225 + 37.37 f_o))) / (-0.6722 + f_o)$	01:26:10
uDSR	$3.5495 \cdot 10^{-2}$	$f_o(\langle z \rangle^4 (0.00005494 + 27.61 f_o) + \langle z \rangle^3 (11.167 + f_o(-218.6 + 530.6 f_o)) + \langle z \rangle^2 (-55.18 + f_o(0.0002025 + (0.0001003 - 1932 f_o) f_o)) + f_o^2(0.0004054 + f_o(0.01723 + (0.05632 - 0.00132 f_o) f_o)) + \langle z \rangle (-51.62 + f_o(-0.00009086 + f_o(-779.3 + (2676 - 3437 f_o) f_o))) + \cos(e^{f_o} + \cos(\langle z \rangle)))$	07:17:49

Table 23. Result from benchmarking the cosmological dataset C16. To increase readability, we only include 4 significant digits and for Genetic Engine 3 significant digits.

Cosmological dataset: C17			
Algorithm	MSE	Equation	Runtime
AI-Feynman	$6.4086 \cdot 10^{-1}$	$-0.1432 + (-62.9 + e^{1+\langle z \rangle + \pi}) \Omega_{Q,0}$	08:53:27
DSO	1.5190	$\Omega_{Q,0} - 2 \left(e^{e^{\langle z \rangle}} + 8 \langle z \rangle \right) \Omega_{m,0} (\langle z \rangle + \Omega_{R,0})$	02:19:20
DSR	$5.7490 \cdot 10^{-1}$	$-\langle z \rangle \left(e^{e^{\Omega_{m,0}} + \sqrt{\Omega_{m,0}} + \sin(\sqrt{\langle z \rangle}) + \sin(\Omega_{m,0})} + 3\Omega_{m,0} \right)$	01:21:24
FFX	$1.6484 \cdot 10^{-1}$	$-12\Omega_{m,0} \max(0, -0.73 + \langle z \rangle)$ $0.37 + \max(0, -0.47 + \langle z \rangle)$ $(-20\Omega_{m,0} - 15 \max(0, -0.22 + \Omega_{m,0}))$ $41 \langle z \rangle \Omega_{m,0} + \max(0, -0.2 + \langle z \rangle)$ $(-21\Omega_{m,0} - 0.34 \max(0, -0.22 + \Omega_{m,0}))$	00:00:29
Genetic Engine	$5.1602 \cdot 10^{-2}$	$\left(-\langle z \rangle^3 \Omega_{Q,0}^4 - 0.1\Omega_{Q,0}^4 - 0.1 \langle z \rangle \Omega_{m,0} \Omega_{Q,0}^2 - \langle z \rangle^4 \Omega_{m,0} \Omega_{Q,0}^2 + \langle z \rangle^{0.072} \Omega_{R,0}^2 \Omega_{m,0}^2 (-0.00052 + 0.11\Omega_{Q,0}) (\Omega_{m,0} + \Omega_{Q,0}) + \langle z \rangle^{5.1} \Omega_{m,0}^3 \Omega_{R,0}^2 \times (-0.47 + 100\Omega_{Q,0}) + (-0.0052 + 1.1\Omega_{Q,0} + \Omega_{m,0} (\Omega_{m,0} + \Omega_{Q,0}) (-0.47 + 100\Omega_{Q,0})) \times \langle z \rangle^{4.1} \Omega_{m,0}^2 \Omega_{R,0}^2 + \langle z \rangle^{1.1} \Omega_{m,0} \Omega_{R,0} \Omega_{Q,0}^2 ((\Omega_{m,0} \times (0.0047 - \Omega_{Q,0}) + 0.0047\Omega_{Q,0}) + \Omega_{R,0} \Omega_{m,0} \times (-0.00052 + 0.11\Omega_{Q,0} + \Omega_{m,0} (\Omega_{m,0} + \Omega_{Q,0})) \times (-0.047 + 10\Omega_{Q,0})) + \langle z \rangle^{2.1} \Omega_{m,0} \Omega_{R,0} \Omega_{m,0}^2 \times (0.0047\Omega_{m,0} \Omega_{Q,0} + (0.0047 - \Omega_{Q,0}) \Omega_{Q,0}^2 + (0.0047 - \Omega_{Q,0} - 0.047\Omega_{R,0} + 10\Omega_{Q,0} \Omega_{R,0})) + \langle z \rangle^{3.1} \Omega_{m,0}^2 \Omega_{R,0} (0.0047 - 0.0052\Omega_{m,0} \Omega_{R,0} + (-1 + (-0.0052 + 1.1\Omega_{m,0} + 1.1\Omega_{Q,0}) \Omega_{R,0}) \times \Omega_{Q,0}) \right) \times \frac{\sqrt{ \langle z \rangle + \Omega_{m,0} }}{\langle z \rangle^{0.072} (0.1 + \langle z \rangle^3) \Omega_{m,0}^2 (\langle z \rangle \Omega_{m,0} + \Omega_{Q,0}^2) \Omega_{R,0}^2}$	04:00:03
GPZGD	$3.6682 \cdot 10^{-2}$	$-9.586 + 8.23(0.02594(6.164 + \langle z \rangle)(-0.3166 + 0.8924\Omega_{m,0} + \Omega_{R,0})(16.74 \langle z \rangle + \sin(\Omega_{Q,0})) + \sin(0.1348 + 2.183\Omega_{m,0} + 2.582\Omega_{R,0}))$	04:00:14
ITEA	$3.5506 \cdot 10^{-2}$	$0.1305 e^{\frac{\langle z \rangle}{\Omega_{m,0}^5 \Omega_{Q,0}^5 \Omega_{R,0}^4}} - 76.3 \sin\left(\frac{\langle z \rangle^2 \Omega_{Q,0}^2}{\Omega_{m,0} \Omega_{R,0}}\right) - 29.53 \left \frac{\langle z \rangle \Omega_{m,0}^{3/2}}{\sqrt{\Omega_{Q,0}}} \right + 0.1504 \cos\left(\frac{\Omega_{m,0}}{\Omega_{Q,0} \Omega_{R,0}^4}\right) + 3.291 \sin\left(\frac{\langle z \rangle^2 \Omega_{m,0}^5 \Omega_{R,0}^2}{\Omega_{Q,0}^3}\right) - 0.04571$	00:59:18
PySR	$4.7813 \cdot 10^{-2}$	$\langle z \rangle - 41.032 \langle z \rangle (1 + \langle z \rangle) \Omega_{m,0}$	01:25:56
QLattice	$3.5840 \cdot 10^{-2}$	$-0.1032 + \Omega_{Q,0}(-0.00791 + 0.00792\Omega_{R,0}) - 0.02986\Omega_{R,0} + \langle z \rangle(-108.6 + \Omega_{Q,0}(28.78 - 28.81\Omega_{R,0}) + 108.7\Omega_{R,0}) + \langle z \rangle^2(-129.8 + \Omega_{Q,0}(34.4 - 34.43\Omega_{R,0}) + 129.9\Omega_{R,0})$	01:26:15
uDSR	3.0153	$e^{e^{(\Omega_{R,0} + \cos(\Omega_{R,0}))} \langle z \rangle} \Omega_{Q,0}$	06:20:17

Table 24. Result from benchmarking the cosmological dataset C17. To increase readability, we only include 4 significant digits and for Genetic Engine and FFX 2 significant digits.

Cosmological dataset: C18

Algorithm	MSE	Equation	Runtime
AI-Feynman	7.1095	$15.06 - e^{1+\langle z \rangle \sin(\Omega_{m,0})}$	08:53:28
DSO	$7.6305 \cdot 10^{-1}$	$-\langle z \rangle (1 + e^{\langle z \rangle} + 4\Omega_{m,0} + \Omega_{R,0} + \Omega_{m,0}) + \Omega_{Q,0}$	01:57:03
DSR	$5.6043 \cdot 10^{-1}$	$-e^{\cos(e^{H_D}) + \langle z \rangle + \Omega_{m,0} + \sqrt{\sin(\Omega_{m,0})} + \sin(\Omega_{m,0})} + \langle z \rangle + e^{2e^{\Omega_{m,0}}}$	01:13:09
FFX	$1.6539 \cdot 10^{-1}$	$-1.7 - 13 \langle z \rangle^2 + 0.55\Omega_{m,0}^2 - 0.35\Omega_{R,0} + 13 \langle z \rangle \Omega_{R,0} + (-18 + 220 \langle z \rangle) \ln(\Omega_{R,0})$	00:00:46
Genetic Engine	$3.8997 \cdot 10^{-2}$	$\langle z \rangle \left(\frac{-10^{-5} + 0.01\Omega_{m,0} + 10^{-7}\Omega_{R,0} - 10^{-4}\Omega_{m,0}\Omega_{R,0} + H_D(0.01 - 10\Omega_{m,0} - 10^{-4}\Omega_{R,0} + 0.1\Omega_{m,0}\Omega_{R,0})}{\Omega_{m,0}(-1.1 + \Omega_{R,0})(-11 - 0.99H_D - 9.9H_D\Omega_{R,0}) + \langle z \rangle^2(-0.011 - 0.01H_D\Omega_{R,0}) + \langle z \rangle(0.22 + \Omega_{R,0}(1.1 + 0.2H_D + H_D\Omega_{R,0}))} + \right.$ $\left. \Omega_{Q,0} \left(\frac{-2.2(10^6)^{-4m,0}\langle z \rangle + 0.00011\Omega_{m,0} + 5\langle z \rangle^2(\Omega_{R,0}(-0.00011 - 2 \cdot 10^{-7}H_D - 0.0001H_D\Omega_{R,0}) + \langle z \rangle^2(1.1 \cdot 10^{-7} + 1 \cdot 10^{-7}H_D\Omega_{R,0}) + 4\Omega_{R,0}(0.00011 + 9.9 \cdot 10^{-8}H_D + 0.00099H_D\Omega_{R,0}))}{10^{-7}} \right) + \right.$ $\left. \frac{-1.1 + \Omega_{R,0}(-11 - 0.99H_D - 9.9H_D\Omega_{R,0}) + \langle z \rangle^2(-0.011 - 0.01H_D\Omega_{R,0}) + \langle z \rangle(0.22 + \Omega_{R,0}(1.1 + 0.2H_D + H_D\Omega_{R,0}))}{(10^{-4} - 0.1\Omega_{m,0})\Omega_{R,0} + H_D(10 - 10^4\Omega_{m,0} - 0.1\Omega_{R,0} - 100\Omega_{m,0}\Omega_{R,0})} + \right.$ $\left. \frac{\Omega_{m,0}(-1.1 + \Omega_{R,0})(-11 - 0.99H_D - 9.9H_D\Omega_{R,0}) + \langle z \rangle^2(-0.011 - 0.01H_D\Omega_{R,0}) + \langle z \rangle(0.22 + \Omega_{R,0}(1.1 + 0.2H_D + H_D\Omega_{R,0}))}{0.0001 + 0.1\Omega_{m,0} + H_D(-0.1 - 100\Omega_{m,0} + 0.001\Omega_{m,0}\Omega_{R,0})} + \right.$ $\left. H_D \left(\frac{11 + \langle z \rangle^2(0.011 + \Omega_{R,0}(-0.011 + 0.01H_D\Omega_{R,0})) + \Omega_{R,0}(9.8 - 11\Omega_{m,0} + H_D(0.99 + (8.9 - 9.9\Omega_{R,0})\Omega_{R,0})) + \langle z \rangle(-0.22 + \Omega_{R,0}(-0.88 + 1.1\Omega_{m,0} + H_D(-0.2 + \Omega_{R,0}(-0.8 + \Omega_{R,0})))}{10^{-5}\Omega_{R,0}} \right) + \right.$ $\left. \frac{1.1 + \langle z \rangle^2(0.0011 + \Omega_{R,0}(-0.0011 + 0.01H_D - 0.01H_D\Omega_{R,0})) + 4\Omega_{R,0}(9.8 - 11\Omega_{m,0} + H_D(0.99 + (8.9 - 9.9\Omega_{R,0})\Omega_{R,0})) + \langle z \rangle(-0.2189 + \Omega_{R,0}(-0.8811 + 1.1\Omega_{m,0} + H_D(-0.89 + 4\Omega_{R,0}(-0.8011 + 4\Omega_{R,0})))}{10^{-5}\Omega_{R,0}} \right)$	04:00:02
GPZGD	$7.0133 \cdot 10^{-3}$	$-9.586 + 8.23((1.713 + H_D)(-2.778 + \Omega_{m,0} + 0.4214\Omega_{Q,0}) - \sin(5.654 + 0.4461 \langle z \rangle) + 0.2646(4.372 - H_D + \Omega_{m,0} + 2.664\Omega_{Q,0} + \langle z \rangle)(3.285 + \Omega_{Q,0}))(3.639 + \Omega_{R,0} + 3.78 \sin(0.0206\Omega_{m,0}))$	04:00:03
ITEA	$1.7350 \cdot 10^{-3}$	$-213.7 + \frac{15.29 - \frac{2.444 \langle z \rangle \Omega_{m,0}^5 \Omega_{R,0}^4}{\Omega_{Q,0}^5}}{H_D} + 68.17 \sqrt{\frac{\langle z \rangle^5 \Omega_{m,0}^5 \Omega_{Q,0}^2}{H_D \Omega_{R,0}^3}}$	00:54:12
PySR	$4.7813 \cdot 10^{-2}$	$23040 \sqrt{\langle z \rangle^2 H_D^3 \Omega_{m,0}^4 \Omega_{Q,0}^4 \Omega_{R,0}^5} + 21.83 \sin\left(\frac{\langle z \rangle^2 \Omega_{m,0}^4 \Omega_{R,0}^5}{\Omega_{Q,0}^2}\right)$	01:29:18
QLattice	$4.0532 \cdot 10^{-3}$	$\langle z \rangle (1 + (-41.03 - 41.03 \langle z \rangle) \Omega_{m,0}) - 73.54 + 201.7 \exp(H_D(0.2235 - 200.3H_D + 0.01824\Omega_{m,0})) + 0.00149\Omega_{m,0} + \langle z \rangle (1.1 + 13.47H_D - 1.238\Omega_{m,0} - 15.17H_D\Omega_{m,0})$	01:25:54
uDSR	3.7302	$1 - e^{e^{-H_D \langle z \rangle + \Omega_{m,0}}}$	05:35:10

Table 25. Result from benchmarking the cosmological dataset C18. To increase readability, we only include 4 significant digits and for Genetic Engine and FFX 2 significant digits.

Cosmological dataset: C19			
Algorithm	MSE	Equation	Runtime
AI-Feynman	$1.5504 \cdot 10^{-3}$	$-23.05 + 23.14 \cos(\sqrt{\langle z \rangle})^{\Omega_{m,0}}$	08:53:26
DSO	$7.7612 \cdot 10^{-4}$	$\langle z \rangle \Omega_{R,0}(-\langle z \rangle - 14\Omega_{m,0} + \Omega_{R,0})$	01:34:04
DSR	$9.0970 \cdot 10^{-3}$	$\sqrt{\Omega_{m,0}}(-2\langle z \rangle - 2\Omega_{m,0} - \sqrt{\langle z \rangle^2}(e^{e^{\Omega_{m,0}}} + \langle z \rangle + \Omega_{m,0}) + \Omega_{R,0})$	01:25:18
FFX	$3.4198 \cdot 10^{-3}$	$0.00905 - 0.406 \langle z \rangle^2 - 11 \langle z \rangle \Omega_{m,0}$	00:00:28
Genetic Engine	$7.3665 \cdot 10^{-4}$	$(\langle z \rangle^2 (\sqrt{ 0.1 + \Omega_{m,0} }(\langle z \rangle (0.0002\Omega_{Q,0} + 2 \cdot 10^{-7} + \langle z \rangle (0.0002 + 0.2\Omega_{Q,0})) \ln(1 + \Omega_{Q,0}^{1/4}) + (10^{-6}\Omega_{Q,0} + \langle z \rangle (10^{-6} + 10^{-3}\Omega_{Q,0} + \langle z \rangle (10^{-5} + 0.01\Omega_{Q,0} + \langle z \rangle (0.01 + 10\Omega_{Q,0})))) \ln(1 + \sqrt{ \Omega_{Q,0} }) + \langle z \rangle (\langle z \rangle (\Omega_{m,0}(1.3 \cdot 10^{-7}\Omega_{Q,0} + \langle z \rangle (1.4 \cdot 10^{-7} + 1.3 \cdot 10^{-5}\langle z \rangle + 0.00014\Omega_{Q,0} + 0.013 \langle z \rangle \Omega_{Q,0})) + (\langle z \rangle (1.4 \cdot 10^{-7} + 1.3 \cdot 10^{-5}\langle z \rangle + 0.00014\Omega_{Q,0} + 0.013 \langle z \rangle \Omega_{Q,0}))\Omega_{R,0}) \ln(1 + \Omega_{Q,0}^{1/4}) + (\Omega_{m,0}(\langle z \rangle (6.9 \cdot 10^{-7}\Omega_{Q,0} + \langle z \rangle (6.9 \cdot 10^{-8} + 0.000069\Omega_{Q,0} + \langle z \rangle (6.9 \cdot 10^{-6} + 0.00063 \langle z \rangle + 0.0069\Omega_{Q,0} + 0.63 \langle z \rangle \Omega_{Q,0})))) + (\langle z \rangle (8.2 \cdot 10^{-7}\Omega_{Q,0} + \langle z \rangle (6.9 \cdot 10^{-8} + 0.000069\Omega_{Q,0} + \langle z \rangle (6.9 \cdot 10^{-6} + 0.00063 \langle z \rangle + 0.0069\Omega_{Q,0} + 0.63 \langle z \rangle \Omega_{Q,0}))))\Omega_{R,0}) \ln(1 + \sqrt{ \Omega_{Q,0} }))) / ((10^{-4} + \langle z \rangle (0.02 + \langle z \rangle)) \times \ln(1 + \sqrt{ \Omega_{Q,0} }) (0.02 \langle z \rangle \ln(1 + \Omega_{Q,0}^{1/4}) + ((10^{-4} + \langle z \rangle^2) \ln(1 + \sqrt{ \Omega_{Q,0} })))$	04:00:03
GPZGD	$1.5285 \cdot 10^{-4}$	$-1.746 + 1.318(0.8415 + (1.941 + \langle z \rangle)(0.2641 - 0.002928\Omega_{m,0})(-1.543 - 0.2123 \langle z \rangle + \Omega_{Q,0}) - \sin(0.3728 \langle z \rangle + 0.01074\Omega_{Q,0}))$	04:00:11
ITEA	$1.1186 \cdot 10^{-4}$	$6.186e^{\langle z \rangle^2 \Omega_{Q,0} \Omega_{R,0}} - 1.437e^{\langle z \rangle^4 \Omega_{Q,0}^2 \Omega_{R,0}^5} - 11.66\sqrt{ \langle z \rangle^5 \Omega_{m,0}^5 \Omega_{Q,0}^2 \Omega_{R,0}^3 } - 4.755 - 1.134\sqrt{\left \frac{\langle z \rangle \Omega_{Q,0}^5 \Omega_{R,0}^5}{\Omega_{m,0}^2}\right } - 4.345 \sin\left(\frac{\langle z \rangle \Omega_{m,0}^3}{\Omega_{Q,0}^2}\right)$	00:54:27
PySR	$1.4803 \cdot 10^{-4}$	$(-9.912 - 3.37 \langle z \rangle \Omega_{R,0}) \sin(\langle z \rangle \Omega_{m,0})$	01:22:57
QLattice	$1.1614 \cdot 10^{-4}$	$(-12.92 + 0.3649\Omega_{Q,0}) \tanh(0.00002407 + \langle z \rangle (0.0035 + \langle z \rangle (0.0013 + 0.2688\Omega_{m,0}) + 0.7258\Omega_{m,0}) + 0.00499\Omega_{m,0}) + 0.00807$	01:35:58
uDSR	$3.8329 \cdot 10^{-2}$	$\langle z \rangle \Omega_{Q,0}(15.15 + \Omega_{R,0})$	06:07:04

Table 26. Result from benchmarking the cosmological dataset C19. To increase readability, we only include 4 significant digits and for Genetic Engine 2 significant digits.

References

- [1] Z. Xu, “Dark matter halo mass functions and density profiles from mass and energy cascade,” *Scientific Reports*, vol. 13, Oct. 2023.
- [2] A. Sonnenfeld, “A robust two-parameter description of the stellar profile of elliptical galaxies,” *Astronomy & Astrophysics*, vol. 641, p. A143, Sept. 2020.
- [3] D. J. Bartlett, L. Kammerer, G. Kronberger, H. Desmond, P. G. Ferreira, B. D. Wandelt, B. Burlacu, D. Alonso, and M. Zennaro, “A precise symbolic emulator of the linear matter power spectrum,” 2023.
- [4] D. J. Bartlett, B. D. Wandelt, M. Zennaro, P. G. Ferreira, and H. Desmond, “syren-halofit: A fast, interpretable, high-precision formula for the Λ CDM nonlinear matter power spectrum,” 2024.
- [5] S. M. Kocsibang, “Machine learning cosmic backreaction and its effects on observations,” *Physical Review Letters*, vol. 130, May 2023.
- [6] S. M. Kocsibang, “Cosmic backreaction and the mean redshift drift from symbolic regression,” *Physical Review D*, vol. 107, May 2023.
- [7] S.-M. Udrescu and M. Tegmark, “Ai feynman: A physics-inspired method for symbolic regression,” *Science Advances*, vol. 6, no. 16, p. eaay2631, 2020.
- [8] S.-M. Udrescu, A. Tan, J. Feng, O. Neto, T. Wu, and M. Tegmark, “Ai feynman 2.0: Pareto-optimal symbolic regression exploiting graph modularity,” 2020.
- [9] B. Burlacu, G. Kronberger, and M. Kommenda, “Operon c++: an efficient genetic programming framework for symbolic regression,” *Proceedings of the 2020 Genetic and Evolutionary Computation Conference Companion*, 2020.
- [10] W. L. Cava, P. Orzechowski, B. Burlacu, F. O. de Franca, M. Virgolin, Y. Jin, M. Kommenda, and J. H. Moore, “Contemporary symbolic regression methods and their relative performance,” 2021.
- [11] B. Burlacu, “Gecco’2022 symbolic regression competition: Post-analysis of the operon framework,” in *Proceedings of the Companion Conference on Genetic and Evolutionary Computation*, GECCO ’23 Companion, (New York, NY, USA), p. 2412–2419, Association for Computing Machinery, 2023.
- [12] J. D. Romano, T. T. Le, W. L. Cava, J. T. Gregg, D. J. Goldberg, N. L. Ray, P. Chakraborty, D. Himmelstein, W. Fu, and J. H. Moore, “Pmlb v1.0: An open source dataset collection for benchmarking machine learning methods,” 2021.
- [13] R. S. Olson, W. L. Cava, P. Orzechowski, R. J. Urbanowicz, and J. H. Moore, “Pmlb: A large benchmark suite for machine learning evaluation and comparison,” 2017.
- [14] N. Makke and S. Chawla, “Interpretable scientific discovery with symbolic regression: A review,” 2023.
- [15] M. Cranmer, “Interpretable machine learning for science with pysr and symbolicregression.jl,” 2023.
- [16] R. P. Feynman, R. B. Leighton, and M. Sands, *The Feynman lectures on physics; New millennium ed.* New York, NY: Basic Books, 2010. Originally published 1963-1965.
- [17] W. Tenachi, R. Iyata, and F. I. Diakogiannis, “Deep symbolic regression for physics guided by units constraints: toward the automated discovery of physical laws,” 2023.
- [18] D. J. Bartlett, H. Desmond, and P. G. Ferreira, “Exhaustive symbolic regression,” *IEEE Transactions on Evolutionary Computation*, p. 1–1, 2023.

- [19] R. Jimenez and A. Loeb, “Constraining cosmological parameters based on relative galaxy ages,” *The Astrophysical Journal*, vol. 573, p. 37–42, July 2002.
- [20] A. Renzini, “Stellar population diagnostics of elliptical galaxy formation,” *Annual Review of Astronomy and Astrophysics*, vol. 44, p. 141–192, Sept. 2006.
- [21] M. Moresco, R. Jimenez, L. Verde, L. Pozzetti, A. Cimatti, and A. Citro, “Setting the stage for cosmic chronometers. i. assessing the impact of young stellar populations on hubble parameter measurements,” *The Astrophysical Journal*, vol. 868, p. 84, Nov. 2018.
- [22] M. Moresco, R. Jimenez, L. Verde, A. Cimatti, and L. Pozzetti, “Setting the stage for cosmic chronometers. ii. impact of stellar population synthesis models systematics and full covariance matrix,” *The Astrophysical Journal*, vol. 898, p. 82, July 2020.
- [23] J. A. Frieman, M. S. Turner, and D. Huterer, “Dark energy and the accelerating universe,” *Annual Review of Astronomy and Astrophysics*, vol. 46, p. 385–432, Sept. 2008.
- [24] A. R. Sandage, “The change of redshift and apparent luminosity of galaxies due to the deceleration of selected expanding universes.,” *The Astrophysical Journal*, vol. 136, p. 319, 1962.
- [25] G. C. Mcvittie, “Appendix to the change of redshift and apparent luminosity of galaxies due to the deceleration of selected expanding universes.,” *The Astrophysical Journal*, vol. 136, p. 334, 1962.
- [26] H. R. Klöckner, D. Obreschkow, C. Martins, A. Raccanelli, D. Champion, A. Roy, A. Lobanov, J. Wagner, and R. Keller, “Real time cosmology - a direct measure of the expansion rate of the universe,” 2015.
- [27] Z. Liu, E. Gan, and M. Tegmark, “Seeing is believing: Brain-inspired modular training for mechanistic interpretability,” 2023.
- [28] T. Buchert and S. Räsänen, “Backreaction in late-time cosmology,” *Annual Review of Nuclear and Particle Science*, vol. 62, p. 57–79, Nov. 2012.
- [29] C. Clarkson, G. Ellis, J. Larena, and O. Umeh, “Does the growth of structure affect our dynamical models of the universe? the averaging, backreaction, and fitting problems in cosmology,” *Reports on Progress in Physics*, vol. 74, p. 112901, Oct. 2011.
- [30] G. F. R. Ellis, “Inhomogeneity effects in cosmology,” *Classical and Quantum Gravity*, vol. 28, p. 164001, Aug. 2011.
- [31] G. F. Ellis and T. Buchert, “The universe seen at different scales,” *Physics Letters A*, vol. 347, p. 38–46, Nov. 2005.
- [32] T. Buchert, “On average properties of inhomogeneous cosmologies,” 2000.
- [33] C. Wetterich, “Can structure formation influence the cosmological evolution?,” *Physical Review D*, vol. 67, feb 2003.
- [34] D. J. Schwarz, “Accelerated expansion without dark energy,” 2002.
- [35] S. Räsänen, “Dark energy from back-reaction,” *Journal of Cosmology and Astroparticle Physics*, vol. 2004, p. 003–003, Feb. 2004.
- [36] T. Buchert, “On average properties of inhomogeneous fluids in general relativity: Dust cosmologies,” *General Relativity and Gravitation*, vol. 32, p. 105–125, Jan. 2000.
- [37] T. Buchert, “On average properties of inhomogeneous fluids in general relativity: Perfect fluid cosmologies,” *General Relativity and Gravitation*, vol. 33, p. 1381–1405, Aug. 2001.
- [38] T. Buchert, P. Mourier, and X. Roy, “On average properties of inhomogeneous fluids in general relativity iii: general fluid cosmologies,” *General Relativity and Gravitation*, vol. 52, Mar. 2020.
- [39] S. Räsänen, “Light propagation in statistically homogeneous and isotropic dust universes,” *Journal of Cosmology and Astroparticle Physics*, vol. 2009, p. 011–011, Feb. 2009.

- [40] S. Räsänen, “Light propagation in statistically homogeneous and isotropic universes with general matter content,” *Journal of Cosmology and Astroparticle Physics*, vol. 2010, p. 018–018, Mar. 2010.
- [41] S. RÄSÄNEN, “Cosmological acceleration from structure formation,” *International Journal of Modern Physics D*, vol. 15, p. 2141–2146, Dec. 2006.
- [42] S. Räsänen, “Accelerated expansion from structure formation,” *Journal of Cosmology and Astroparticle Physics*, vol. 2006, p. 003–003, Nov. 2006.
- [43] S. M. Koksang, “Another look at redshift drift and the backreaction conjecture,” *Journal of Cosmology and Astroparticle Physics*, vol. 2019, p. 036–036, Oct. 2019.
- [44] S. M. Koksang, “Observations in statistically homogeneous, locally inhomogeneous cosmological toy-models without flrw backgrounds,” 2020.
- [45] A. Heinesen, “Redshift drift as a model independent probe of dark energy,” *Physical Review D*, vol. 103, Apr. 2021.
- [46] S. M. Koksang, “Searching for signals of inhomogeneity using multiple probes of the cosmic expansion rate $H(z)$,” *Physical Review Letters*, vol. 126, June 2021.
- [47] S.-M. Udrescu and M. Tegmark, “Ai feynman: A physics-inspired method for symbolic regression,” *Science Advances*, vol. 6, no. 16, p. eaay2631, 2020.
- [48] S.-M. Udrescu, A. Tan, J. Feng, O. Neto, T. Wu, and M. Tegmark, “Ai feynman 2.0: Pareto-optimal symbolic regression exploiting graph modularity,” *arXiv preprint arXiv:2006.10782*, 2020.
- [49] B. K. Petersen, M. Landajuela, T. N. Mundhenk, C. P. Santiago, S. K. Kim, and J. T. Kim, “Deep symbolic regression: Recovering mathematical expressions from data via risk-seeking policy gradients,” in *Proc. of the International Conference on Learning Representations*, 2021.
- [50] T. N. Mundhenk, M. Landajuela, R. Glatt, C. P. Santiago, D. M. Faissol, and B. K. Petersen, “Symbolic regression via neural-guided genetic programming population seeding,” in *Advances in Neural Information Processing Systems*, 2021.
- [51] B. K. Petersen, M. L. Larma, T. N. Mundhenk, C. P. Santiago, S. K. Kim, and J. T. Kim, “Deep symbolic regression: Recovering mathematical expressions from data via risk-seeking policy gradients,” in *International Conference on Learning Representations*, 2021.
- [52] T. McConaghy, *FFX: Fast, Scalable, Deterministic Symbolic Regression Technology*, pp. 235–260. New York, NY: Springer New York, 2011.
- [53] G. Espada, L. Ingelse, P. Canelas, P. Barbosa, and A. Fonseca, “Datatypes as a more ergonomic frontend for grammar-guided genetic programming,” in *GPCE ’22: Concepts and Experiences, Auckland, NZ, December 6 - 7, 2022* (B. Scholz and Y. Kameyama, eds.), p. 1, ACM, 2022.
- [54] G. Dick, C. A. Owen, and P. A. Whigham, “Feature standardisation and coefficient optimisation for effective symbolic regression,” in *Proceedings of the 2020 Genetic and Evolutionary Computation Conference, GECCO ’20*, (New York, NY, USA), p. 306–314, Association for Computing Machinery, 2020.
- [55] F. O. de Franca and G. S. I. Aldeia, “Interaction-Transformation Evolutionary Algorithm for Symbolic Regression,” *Evolutionary Computation*, pp. 1–25, 12 2020.
- [56] M. Cranmer, “Interpretable machine learning for science with pysr and symbolicregression.jl,” 2023.
- [57] N. J. Christensen, S. Demharter, M. Machado, L. Pedersen, M. Salvatore, V. Stentoft-Hansen, and M. T. Iglesias, “Identifying interactions in omics data for clinical biomarker discovery using symbolic regression,” *Bioinformatics*, vol. 38, pp. 3749–3758, 06 2022.

- [58] M. Landajuela, C. Lee, J. Yang, R. Glatt, C. P. Santiago, I. Aravena, T. N. Mundhenk, G. Mulcahy, and B. K. Petersen, “A unified framework for deep symbolic regression,” in *Advances in Neural Information Processing Systems*, 2022.
- [59] N. Makke and S. Chawla, “Interpretable scientific discovery with symbolic regression: A review,” 2023.
- [60] W. L. Cava, P. Orzechowski, B. Burlacu, F. O. de França, M. Virgolin, Y. Jin, M. Kommenda, and J. H. Moore, “Contemporary symbolic regression methods and their relative performance,” 2021.
- [61] M. Kommenda, A. Beham, M. Affenzeller, and G. Kronberger, *Complexity Measures for Multi-objective Symbolic Regression*, p. 409–416. Springer International Publishing, 2015.
- [62] E. J. Michaud, Z. Liu, and M. Tegmark, “Precision machine learning,” *Entropy*, vol. 25, p. 175, Jan. 2023.